Infectious Diseases

4

Chen Zhang and Jeffrey L. Myers

Pulmonary infections are caused by a wide range of pathogenic microorganisms, including bacteria, viruses, fungi, and parasites. The most common lung infections in immunocompetent hosts are caused by pyogenic bacteria (e.g., *Streptococcus pneumoniae*), common respiratory viruses, and mycoplasma. These infections are usually diagnosed by clinical and microbiologic studies, including cultures and serology tests. Lung biopsy is rarely used in these diagnoses. Patients with life-threatening pneumonia, especially those who are immunocompromised, are more likely to undergo lung biopsy to rule out unusual infections not easily diagnosed using conventional microbiologic methods and for which treatment strategies may be different. Pathogens more likely to be diagnosed using lung biopsy for which there are characteristic pathologic changes are highlighted in this chapter and listed in Table 4.1.

C. Zhang (✉)
Department of Pathology and Laboratory Medicine, Indiana University School of Medicine, Indianapolis, IN, USA
e-mail: chenzhan@iupui.edu

J. L. Myers
Department of Pathology, Michigan Medicine, Ann Arbor, MI, USA
e-mail: myerjeff@med.umich.edu

C. Zhang, J. L. Myers (eds.), *Atlas of Lung Pathology*, Atlas of Anatomic Pathology,
https://doi.org/10.1007/978-1-4939-8689-7_4

Table 4.1 List of pulmonary infections encountered in lung biopsies, surgical resections, and autopsies

Bacteria (non-mycobacteria)
Community-acquired pneumonia: *Streptococcus pneumoniae*, *Mycoplasma pneumoniae*, *Chlamydia pneumoniae*, *Haemophilus influenzae*
Health care-associated pneumonia with or without resistance risk factors: Drug-resistant *Streptococcus pneumoniae*, *Legionella spp.*, *Haemophilus influenzae*, *Mycoplasma pneumoniae*, *Chlamydia pneumoniae*, enteric gram-negative bacilli
Nocardiosis
Actinomycosis
Rhodococcus equi pneumonia (malakoplakia)
Mycobacteria
Mycobacterium tuberculosis (tuberculosis)
Atypical/nontuberculous mycobacterial infections
Viruses
Cytomegalovirus pneumonia
Herpes simplex virus pneumonia
Adenovirus pneumonia
Measles pneumonia
Respiratory syncytial virus pneumonia
Influenza virus pneumonia
Fungi
Aspergillosis
Mucormycosis
Candidiasis
Cryptococcosis
Histoplasmosis
Blastomycosis
Coccidioidomycosis
Pneumocystis jirovecii
Parasites
Toxoplasmosis
Amoebiasis
Dirofilarial nodule (dog heartworm disease)
Paragonimiasis
Strongyloidiasis

Bacterial Pneumonia

Acute bronchopneumonia (Figs. 4.1, 4.2 and 4.3) is caused by various gram-positive or gram-negative bacteria that are sometimes visible on a Gomori methenamine silver (GMS) stain. Bacterial identification using tissue gram stains has low sensitivity and specificity and is neither necessary nor possible in most cases.

Legionnaires' disease (Fig. 4.4) is an acute bronchopneumonia often characterized by prominent necrosis, karyorrhexis, and histiocyte-rich fibrinous exudates. Special stains are of limited value in identifying the gram-negative bacillus responsible for Legionnaires' disease and have been largely supplanted by a combination of cultures and serology.

Nocardiosis (Fig. 4.5) occurs almost exclusively in immunocompromised patients and is caused by a gram-positive filamentous organism (*Nocardia spp.*) common in soil and as normal oral microflora. *Nocardia* pneumonia may follow a fulminant course, and about half of patients develop disseminated infections, which frequently involve the central nervous system. Actinomycosis (Fig. 4.6) is also caused by gram-positive, anaerobic, filamentous bacteria (*Actinomyces spp.*) common in the oral cavity and oropharynx. Actinomycosis often occurs in patients with poor oral and dental hygiene. Lung involvement frequently includes fistulous involvement of pleural and chest wall soft tissues. Microscopically, the histologic findings are similar to those described in nocardiosis, but the organisms have a propensity to form larger macroscopic colonies in vivo that are identifiable in routinely stained sections as sulfur granules; these are indistinguishable from those seen more commonly in tonsils.

Rhodococcus equi pneumonia (malakoplakia) (Fig. 4.7) is caused by a gram-positive bacillus commonly found in soil. Pulmonary infection occurs primarily in immunocompromised patients, most commonly in AIDS patients but also in other immunocompromised populations and occasionally in immunocompetent adults. The histologic findings unique to malakoplakia are the key to establishing the diagnosis in biopsy specimens.

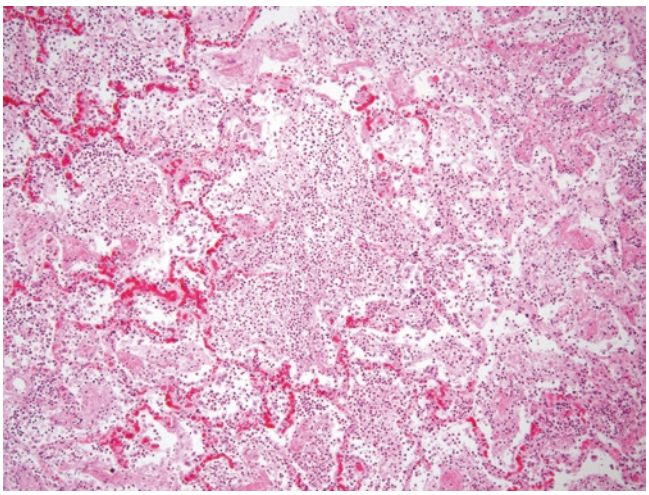

Fig. 4.1 Acute bronchopneumonia. Low-magnification photomicrograph shows an exquisitely air-space-centered process in which acute inflammatory cells and fibrin fill the lumens of distal airways and air spaces. Alveolar septa are congested and focally disrupted, but the overall alveolar structure is preserved

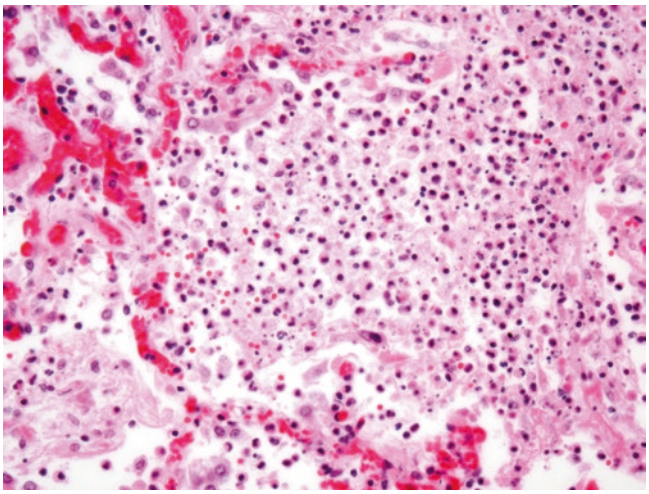

Fig. 4.2 Acute bronchopneumonia. High-magnification photomicrograph shows that the air-space exudate is composed mainly of neutrophils with prominent karyopyknosis and karyorrhexis, histiocytes, and fibrin

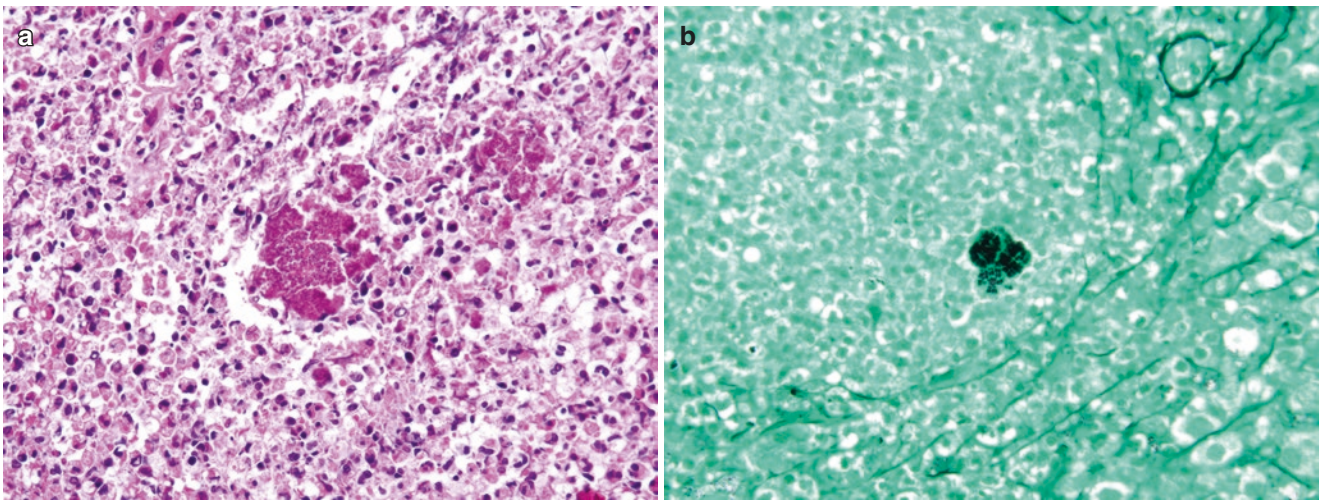

Fig. 4.3 Acute bronchopneumonia. High-magnification photomicrographs showing bacterial colonies of the kind occasionally observed in acute bronchopneumonia on routine H&E (**a**) and GMS (**b**) stains

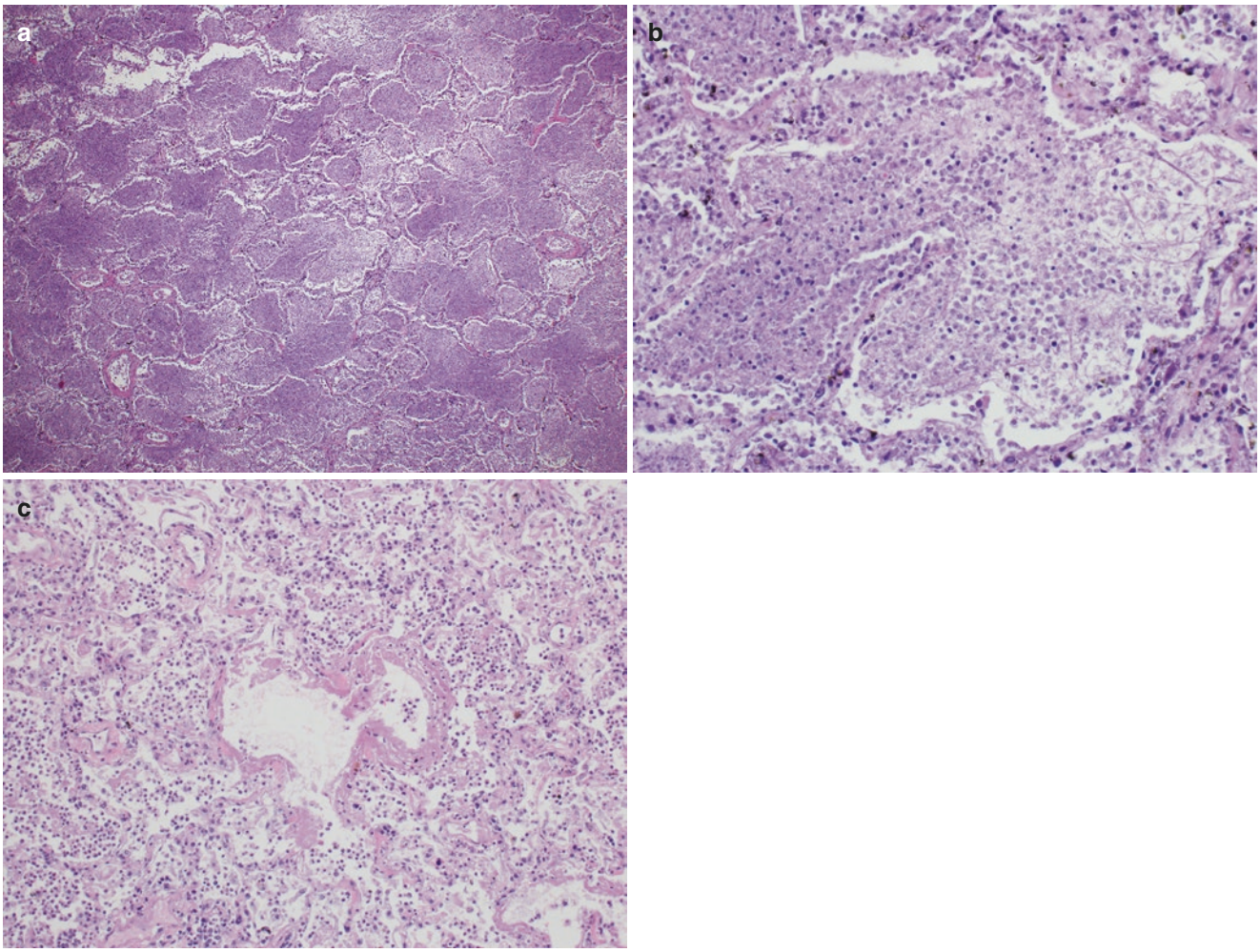

Fig. 4.4 Legionnaires' disease. (**a**) Low-magnification photomicrograph showing acute bronchopneumonia with prominent intra-alveolar fibrinous exudates in a patient with Legionnaires' disease. (**b**) Higher-magnification photomicrograph showing acute bronchopneumonia with prominent necrosis, an inflammatory infiltrate in which histiocytes predominate, and fibrin. (**c**) Intermediate-magnification view of autopsy findings in the same patient illustrating a combination of acute bronchopneumonia and diffuse alveolar damage with well-formed hyaline membranes, a finding characteristic of Legionnaires' disease in a subset of patients

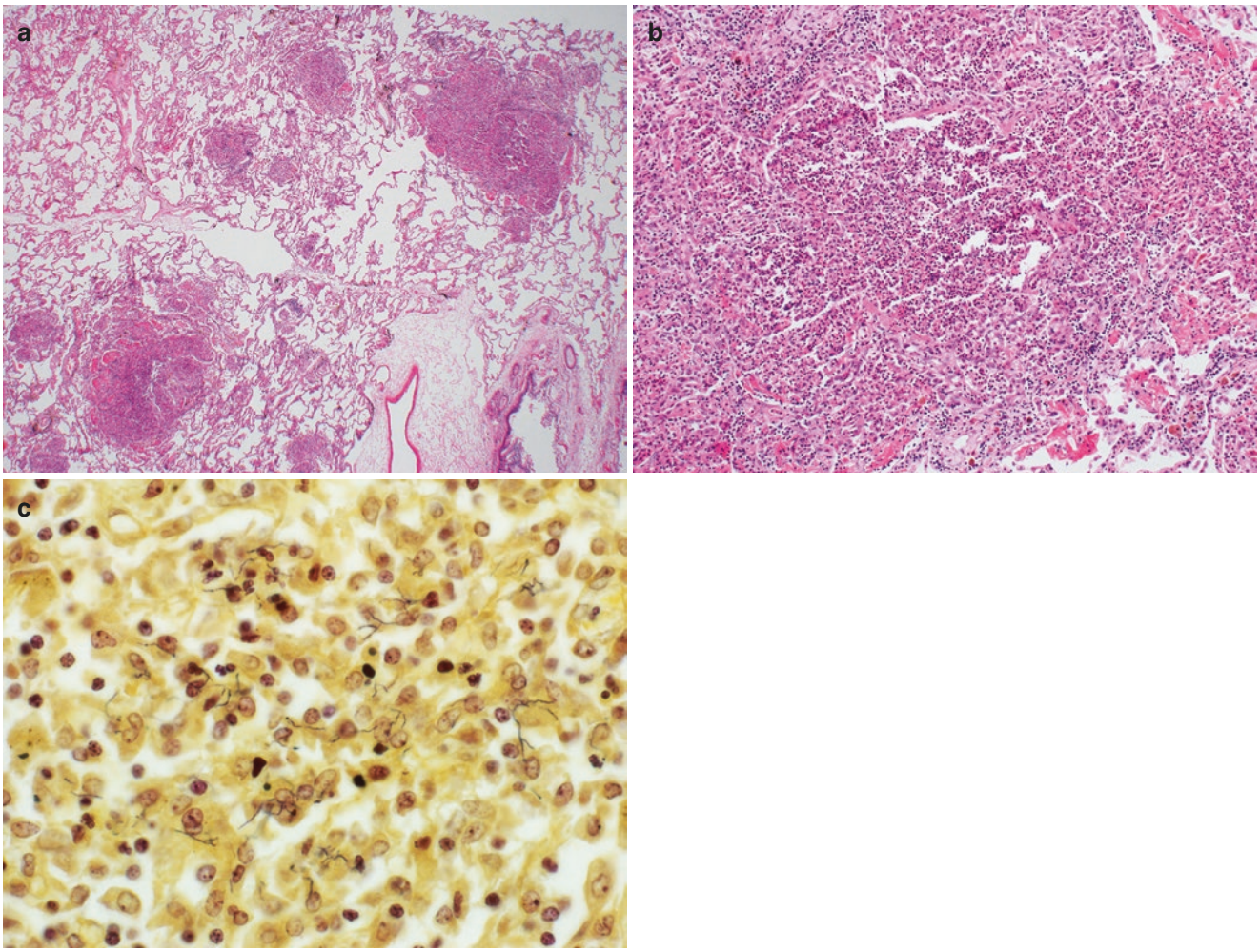

Fig. 4.5 *Nocardia* pneumonia. (**a**) Low-magnification photomicrograph showing a patchy necrotizing acute bronchopneumonia forming circumscribed microabscesses with a vaguely granulomatous appearance. (**b**) Higher-magnification photomicrograph showing a vaguely granulomatous microabscess at higher magnification but without the giant cells, epithelioid macrophages, or associated non-necrotizing granulomas more typical of granulomatous infection. (**c**) High-magnification photomicrograph in which a tissue gram (Brown-Brenn) stain shows the filamentous bacteria typical of *Nocardia spp*.

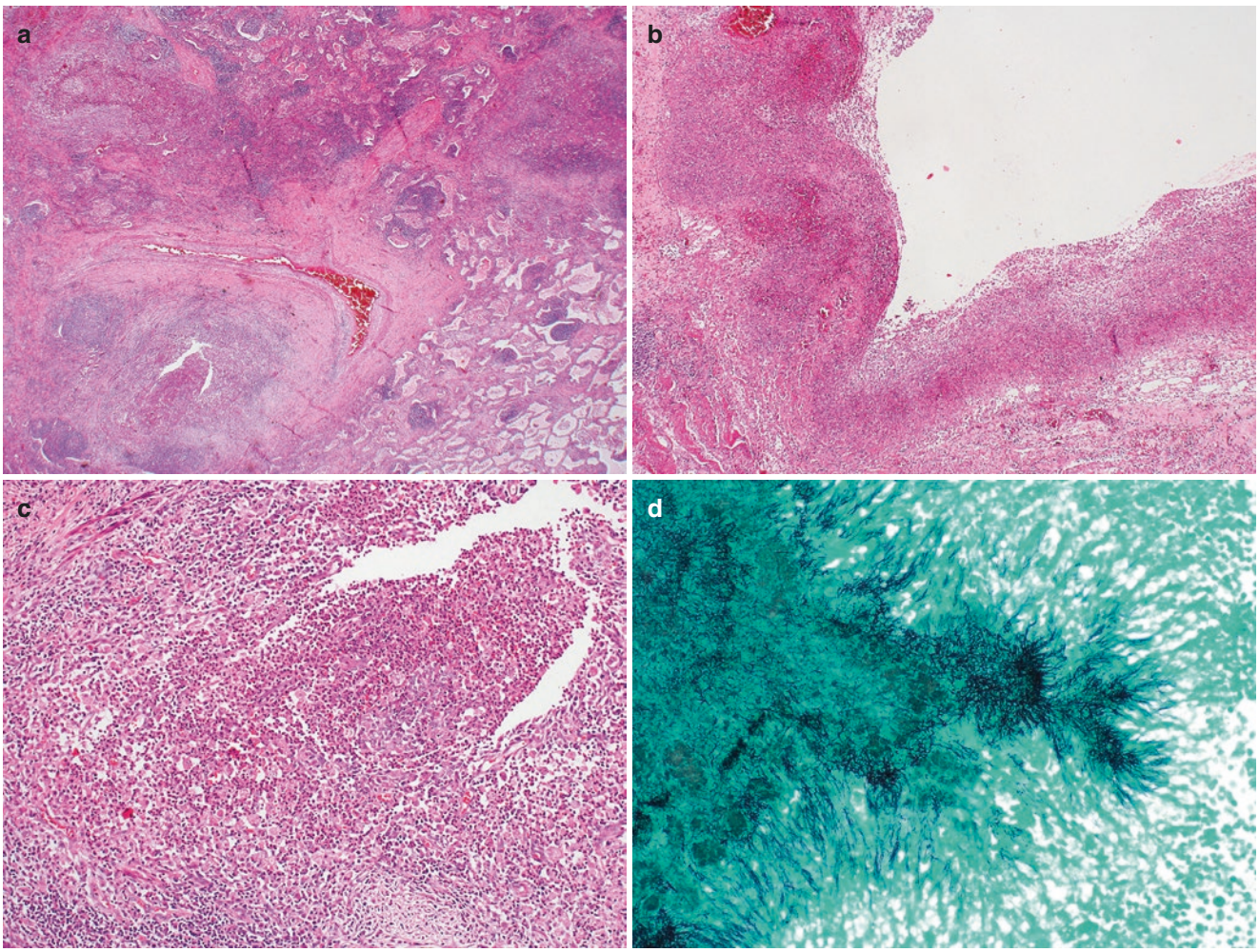

Fig. 4.6 Actinomycosis. (**a**) Low-magnification photomicrograph showing patchy necrotizing acute bronchopneumonia with multifocal microabscesses. (**b**) Low-magnification photomicrograph from the same patient showing a macroscopic abscess with the suppurative inflammation characteristic of actinomycosis. (**c**) Intermediate-magnification photomicrograph showing a circumscribed abscess resembling the vaguely granulomatous microabscesses seen in nocardiosis. (**d**) Intermediate-magnification photomicrograph in which a GMS stain illustrates filamentous *Actinomyces spp.* forming a sulfur granule

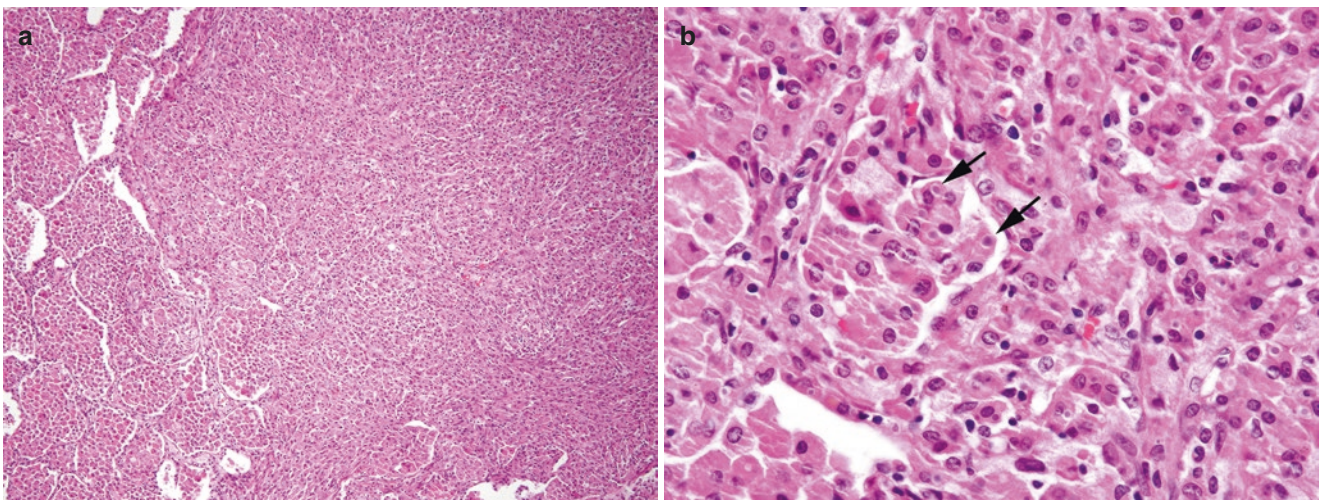

Fig. 4.7 *Rhodococcus equi* pneumonia (malakoplakia). (**a**) Low-magnification photomicrograph showing massive proliferation of histiocytes/macrophages arranged in confluent sheets (right side) and focally filling the alveoli in a pattern mimicking desquamative interstitial pneumonia (left side). Most of the macrophages are round to oval in shape, while others may assume a more spindled appearance. (**b**) High-magnification view shows epithelioid histiocytes with abundant eosinophilic cytoplasm and the intracytoplasmic round basophilic targetoid inclusions (Michaelis-Gutmann bodies) (arrows) diagnostic of malakoplakia. Michaelis-Gutmann bodies are usually easily identified on H&E stain, but calcium stains such as the von Kossa stain may also be helpful in identifying them

Mycobacterial Disease (Figs. 4.8, 4.9, 4.10, 4.11, 4.12 and 4.13)

The prevalence of *Mycobacterium tuberculosis* infection (tuberculosis) is low in the United States. Incident cases have fallen dramatically, and most newly diagnosed cases represent reactivation disease in immigrants who acquired the infection elsewhere. Most cases are diagnosed clinically by means of skin tests, cultures, and other laboratory tests. Occasionally, tuberculosis manifesting as a solitary lung nodule or miliary lesions may be biopsied or resected owing to a preoperative concern for malignancy.

Atypical/nontuberculous mycobacterial infections of the lung (Figs. 4.11, 4.12 and 4.13) commonly resemble tuberculosis in terms of clinical presentations and patterns of disease in both immunocompetent and immunocompromised hosts. Definitive diagnosis relies on culture and molecular techniques. *Mycobacterium avium complex (*MAC*)* is the most commonly encountered nontuberculous mycobacterium. In addition to causing patterns of disease resembling those seen in tuberculosis, MAC also causes a hypersensitivity pneumonia-like syndrome resulting from sensitization to contaminated hot tubs ("hot-tub lung").

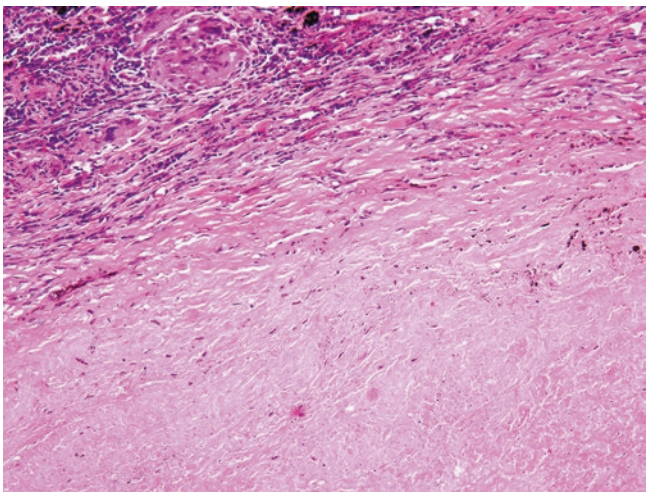

Fig. 4.8 Tuberculosis. Photomicrograph showing characteristic necrotizing (caseating) granuloma with central bland necrosis surrounded by epithelioid histiocytes and multinucleated giant cells. While typical of tuberculosis, this same histology and distribution of disease also occurs in patients with nontuberculous mycobacterial infections

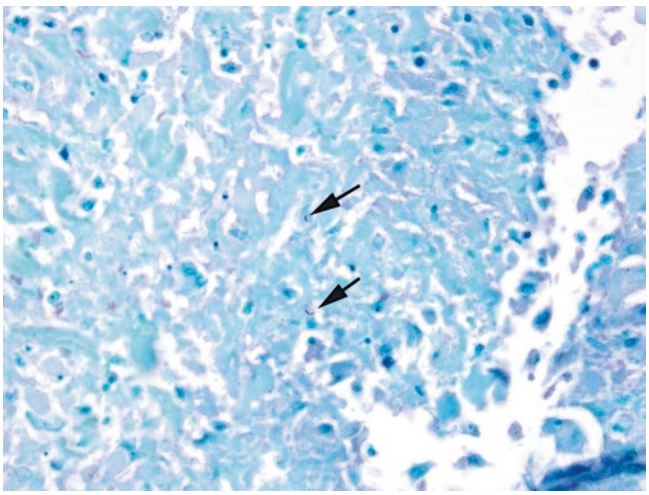

Fig. 4.10 Tuberculosis. High-magnification photomicrograph showing acid-fast organisms (arrows) in a section stained using a Ziehl-Neelsen technique. While there are subtle differences between *Mycobacterium tuberculosis* and nontuberculous mycobacterial organisms, they cannot be reliably separated based on morphology alone; speciation is accomplished more reliably with culture or molecular techniques. The organisms are usually scarce even when necrosis is extensive. Careful examination under high magnification is necessary

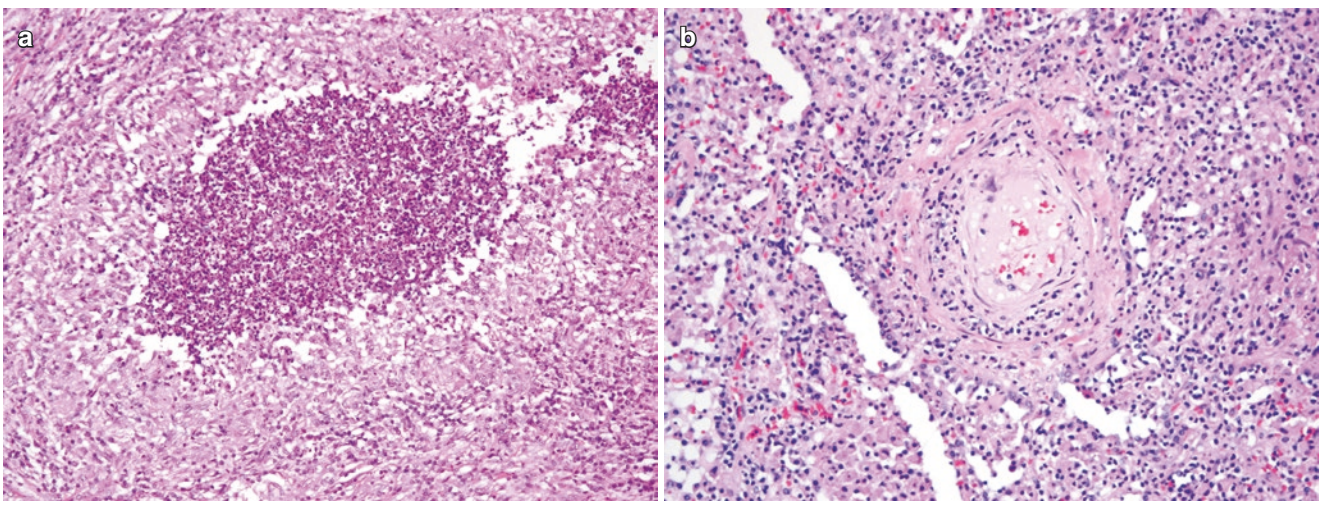

Fig. 4.9 Tuberculosis. Photomicrograph showing a necrotizing granuloma in which central necrosis comprises necrotizing neutrophils. The purulent necrotic center is surrounded by epithelioid histiocytes admixed with lymphocytes and plasma cells (**a**). Occasionally vascular inflammation is prominent, although a true necrotizing vasculitis is rare (**b**)

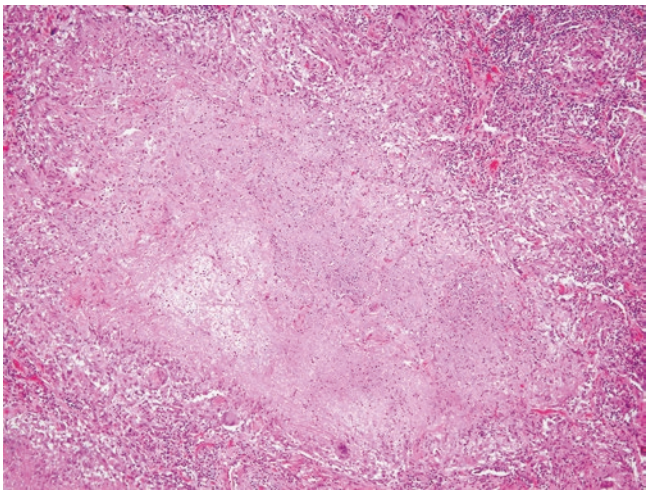

Fig. 4.11 Nontuberculous mycobacteria infection due to MAC. Low-magnification photomicrograph showing necrotizing granulomatous inflammation at autopsy in a patient with culture-proven MAC. The histology strongly suggests granulomatous infection but is not specific to MAC, a diagnosis that requires a combination of special stains, cultures, and molecular techniques

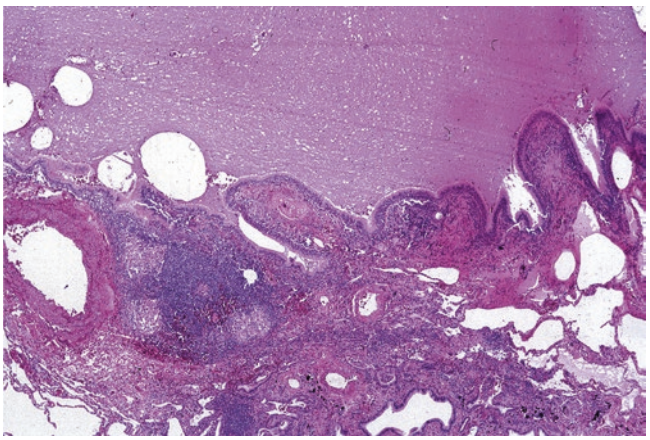

Fig. 4.12 Nontuberculous mycobacterial infection in a patient with bronchiectasis. Low-magnification photomicrograph showing an ectatic airway with severe chronic inflammation typical of bronchiectasis. In this case, the inflammation is complicated by loose non-necrotizing granulomas in the airway wall, a finding virtually diagnostic of atypical mycobacterial infection (usually MAC) in the context of bronchiectasis. This type of atypical mycobacterial infection in the setting of large airway disease is commonly seen in the middle lobe and/or lingula (middle lobe syndrome) but may affect any area of localized bronchiectasis

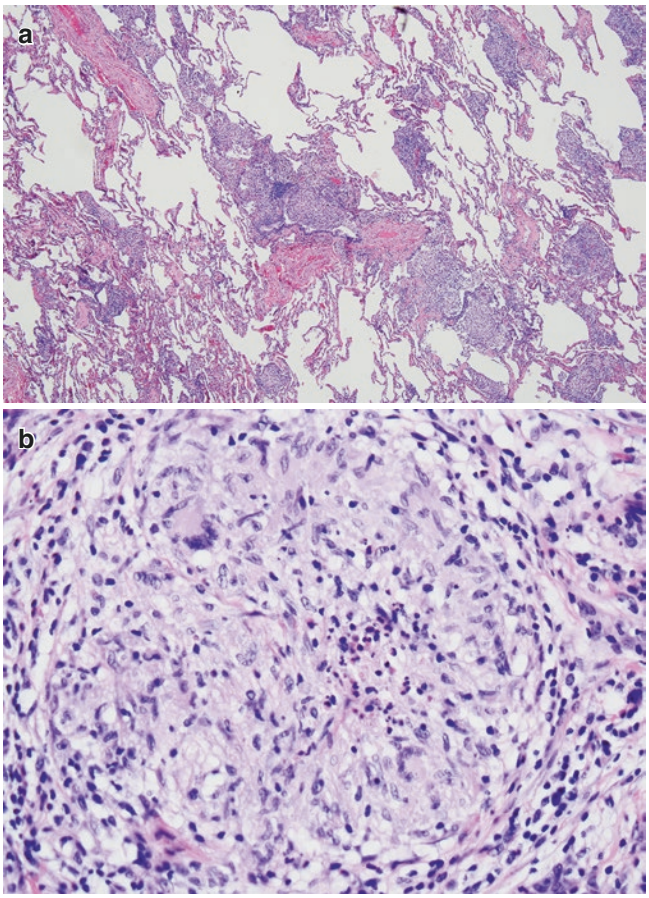

Fig. 4.13 MAC infection in a patient with a hypersensitivity pneumonia-like syndrome linked to hot-tub exposure (hot-tub lung). (**a**) Low-magnification photomicrograph showing a combination of chronic bronchiolitis and relatively well-formed non-necrotizing and focally necrotizing granulomas situated predominantly within the lumens of distal airways. (**b**) Higher magnification view from the same biopsy specimen showing a small focus of central necrosis with neutrophils

Viral Pneumonia

Viral pneumonia is common, especially in immunocompromised patients. Some viral infections cause unique cytopathic changes that can be identified on routinely stained sections (Figs. 4.14, 4.15, 4.16, 4.17, 4.18, 4.19 and 4.20). Immunohistochemical staining with specific antibodies is helpful in identifying some of the viruses with overlapping histologic features with greater confidence.

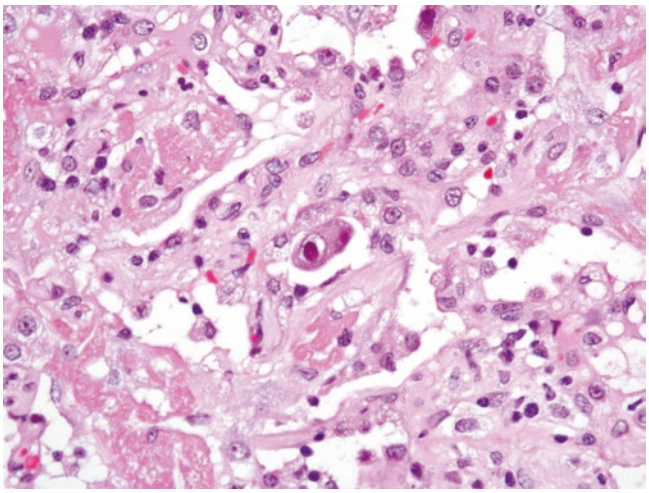

Fig. 4.14 Cytomegalovirus (CMV) pneumonia. High-magnification photomicrograph shows the histologic hallmark of CMV pneumonia, the enlarged cells containing both intranuclear and intracytoplasmic inclusions. The intranuclear inclusion is dark purple and is surrounded by a clear halo (owl's eye). The cytopathic changes are usually seen in bronchiolar epithelium and endothelial cells but may occasionally affect other cells, including macrophages

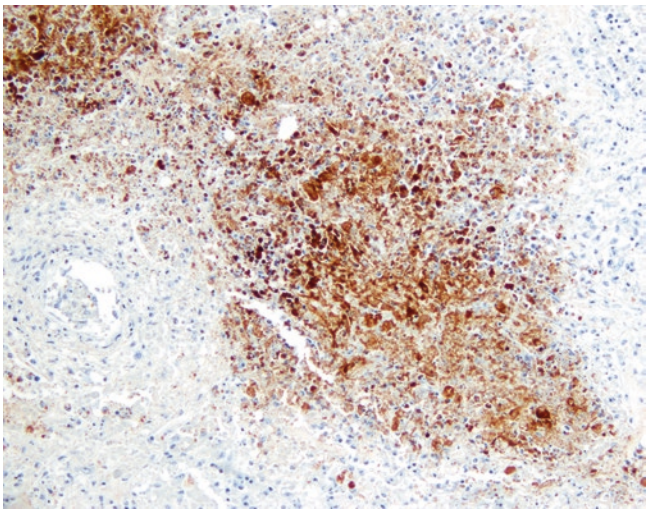

Fig. 4.16 Herpes simplex virus (HSV) pneumonia. Photomicrograph showing positive immunohistochemical staining with HSV-I antibody. Immunostains can be helpful in cases with equivocal or atypical inclusions

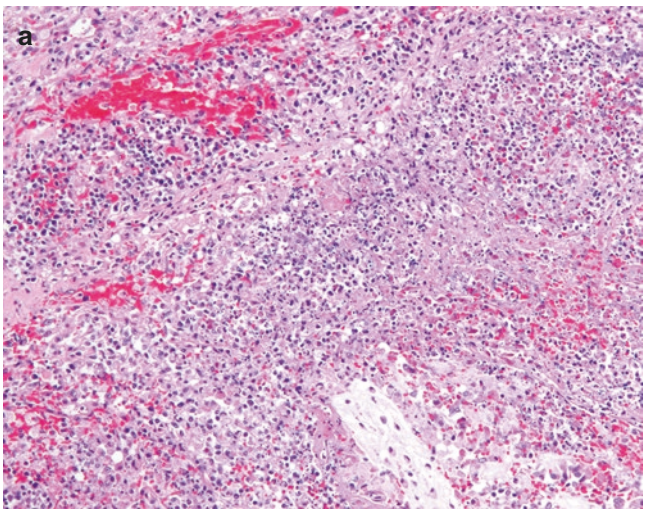

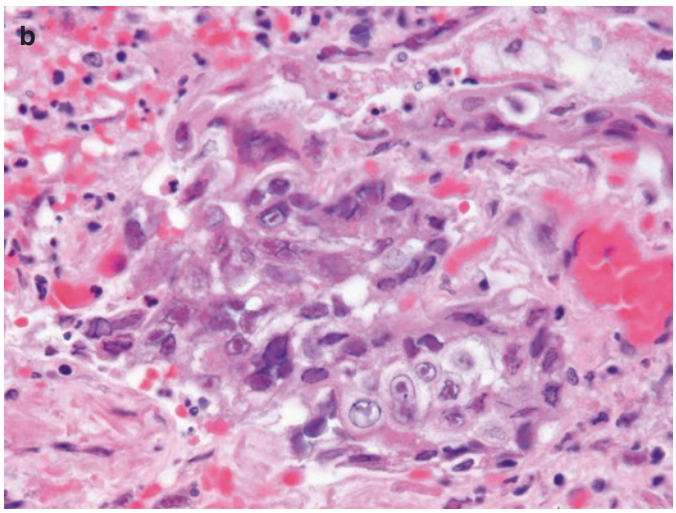

Fig. 4.15 Herpes simplex virus (HSV) pneumonia. (**a**) Photomicrograph showing necrotizing bronchitis and bronchopneumonia with prominent karyorrhexis typical of HSV infection. The bronchiolocentric necrotizing process destroys the airway and surrounding parenchyma. (**b**) High-magnification photomicrograph showing characteristic Cowdry type A inclusions that are round, eosinophilic, and surrounded by a clear halo. Peripheral margination of chromatin is also seen. Other inclusions are characterized by dense, ground-glass change filling up the entire nucleus with a surrounding basophilic rim

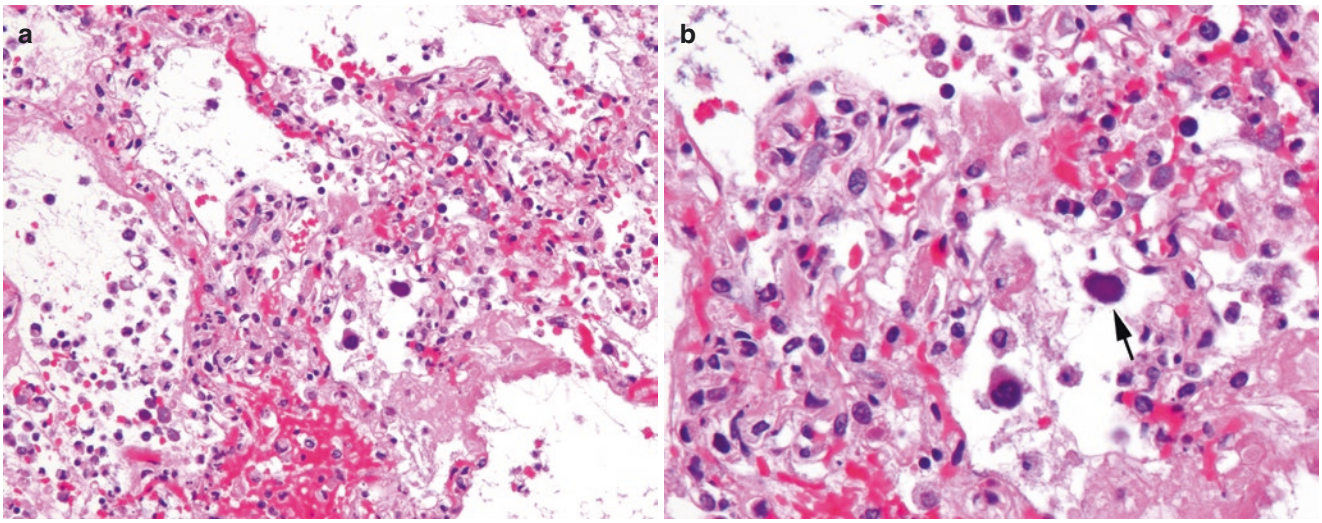

Fig. 4.17 Adenovirus pneumonia. (**a**) Intermediate magnification photomicrograph showing diffuse alveolar damage with hyaline membranes and an associated air-space exudate that includes macrophages, neutrophils, and fibrin. (**b**) High-magnification view demonstrating adenovirus intranuclear inclusion with the typical dark and smudged appearance (arrow)

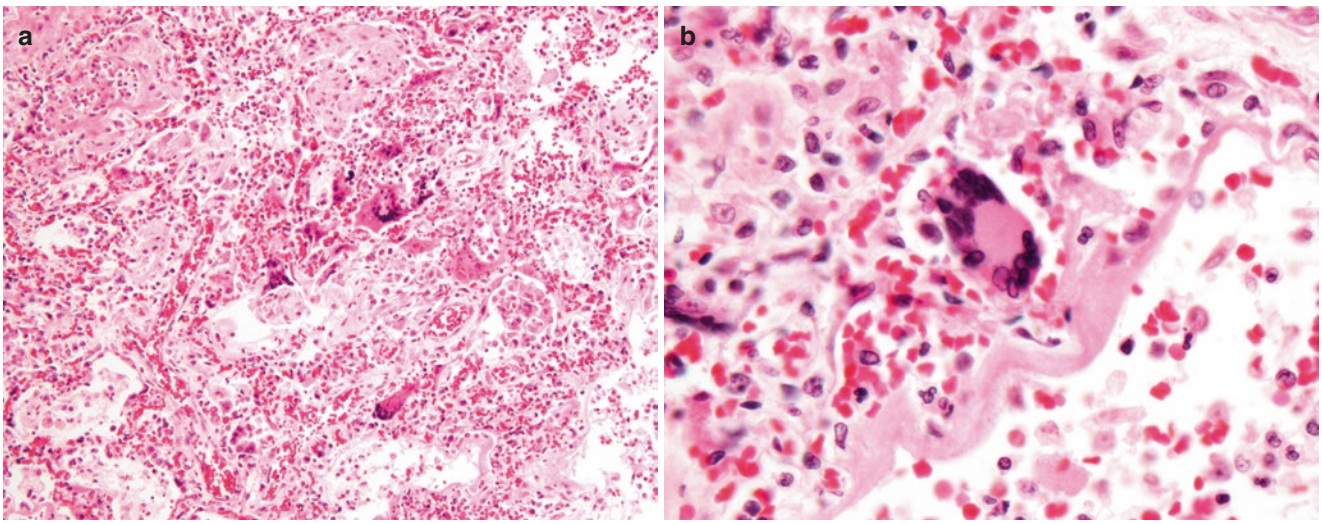

Fig. 4.18 Measles pneumonia. (**a**) Photomicrograph showing numerous large multinucleated giant cells in diffuse alveolar damage. (**b**) High-magnification view of the multinucleated giant cell with intranuclear eosinophilic inclusions and chromatin margination

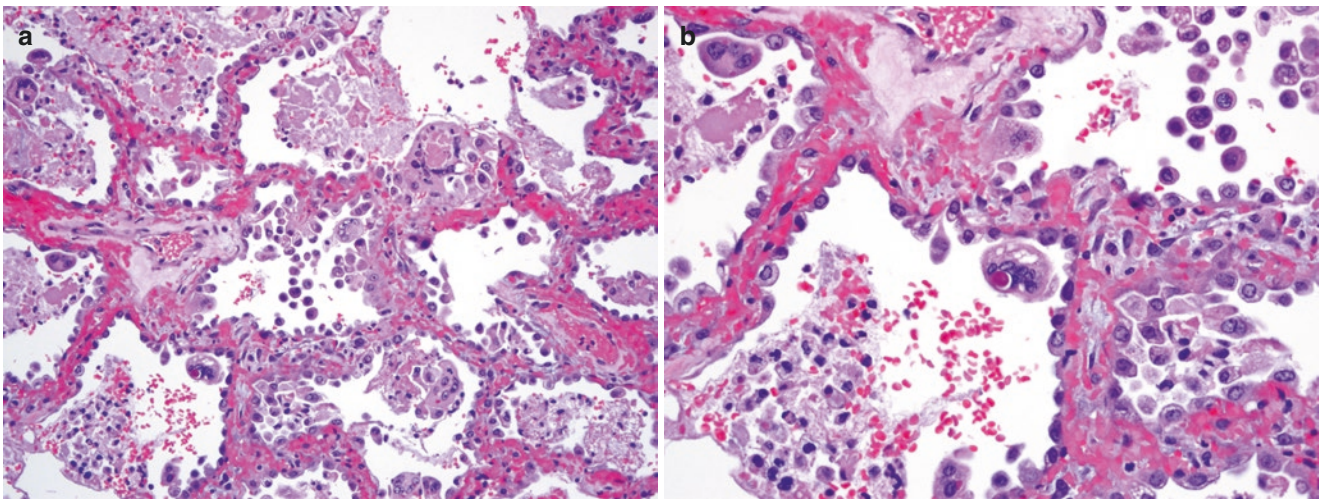

Fig. 4.19 Respiratory syncytial virus (RSV) pneumonia is a significant cause of respiratory disease in children but rarely requires biopsy for diagnosis. (**a**) Photomicrograph of a surgical lung biopsy showing multinucleated giant cells in diffuse alveolar damage with prominent hyperplasia of type 2 pneumocytes. Diffuse alveolar damage (DAD) is a relatively uncommon finding in RSV pneumonia, seen only in those with severe disease. (**b**) High-magnification photomicrograph showing a multinucleated giant cell with round, eosinophilic intracytoplasmic inclusions

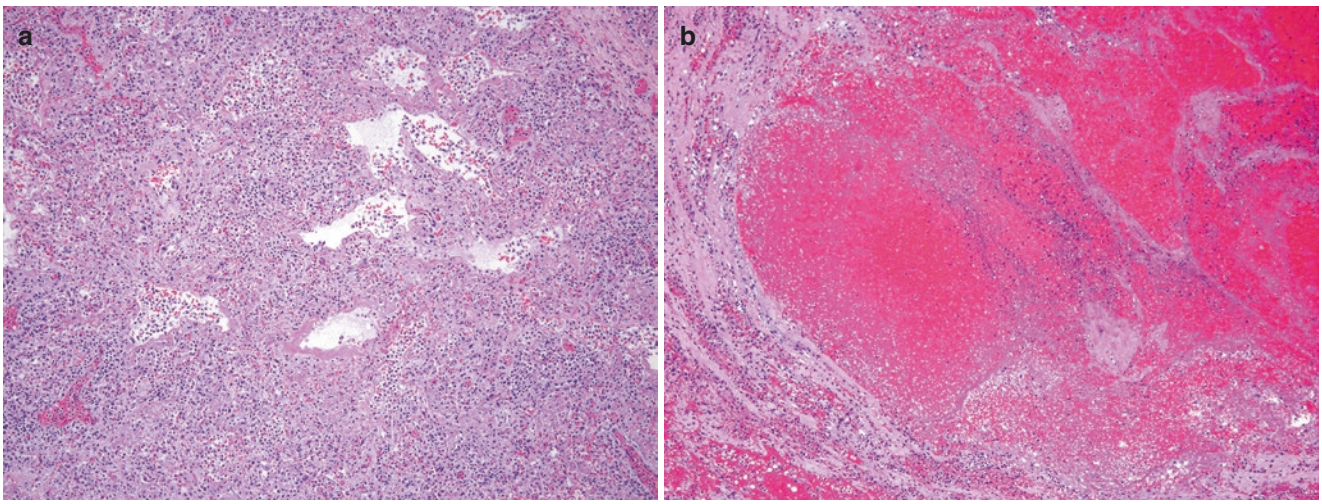

Fig. 4.20 Influenza virus H1N1 pneumonia. (**a**) Low magnification showing a combination of diffuse alveolar damage and a necrotizing inflammatory infiltrate typical of influenza pneumonia. Diagnostic cytopathic changes are absent in influenza pneumonia. (**b**) Low-magnification photomicrograph from the same patient showing a large area of hemorrhagic infarct, a characteristic feature of influenza virus type H1N1 infection

Fungal Pneumonia

The types of fungal infections encountered in lung biopsies or surgical lung specimens are heavily dependent on whether the patient is immunocompetent or immunocompromised. Fungal infections more commonly seen in immunologically intact hosts may also occur in immunocompromised patients in whom the histologic findings may be more variable. Histoplasmosis, blastomycosis, cryptococcosis, and coccidioidomycosis are the fungal infections likely to be encountered in lung biopsies from immunocompetent hosts living in North America. Other fungal diseases are seen almost exclusively in immunocompromised patients.

Histoplasmosis

Histoplasmosis (Figs. 4.21, 4.22, 4.23, 4.24) is endemic in the Mississippi and Ohio River valleys of the United States. The disease is usually asymptomatic and self-limited but may cause a persistent lung nodule that leads to a needle biopsy or excision of the lesion. Necrotizing granulomatous inflammation is the usual finding, except for disseminated histoplasmosis, which is an uncommon form of the disease seen more often in immunocompromised patients.

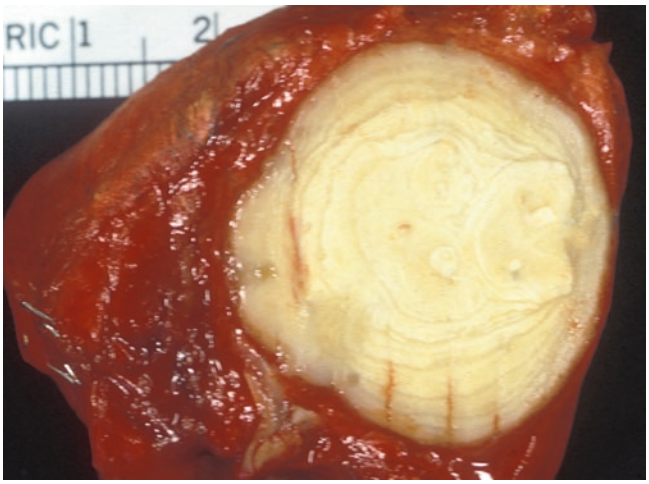

Fig. 4.21 Histoplasmosis. Gross photograph showing cut surface of a well-circumscribed lesion with prominent central necrosis showing concentric rings (resembling the rings of a tree) that are characteristic of histoplasmosis

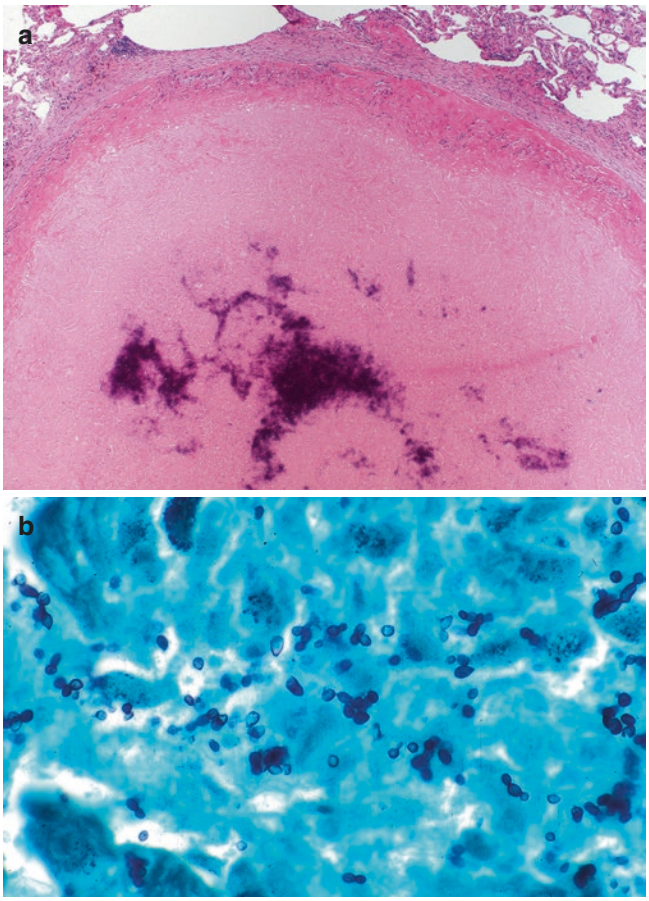

Fig. 4.22 Histoplasmosis. (**a**) Low-magnification photomicrograph of the lesion shown in Fig. 4.21. The lesion shows a rounded border and prominent central necrosis with calcification, surrounded by a thin rim of epithelioid histiocytes and collagen fibrosis. The organisms are few in quantity and are invisible on H&E-stained slides. (**b**) High-magnification photomicrograph of GMS stain showing small, uniform, oval-shaped yeasts with narrow-based budding

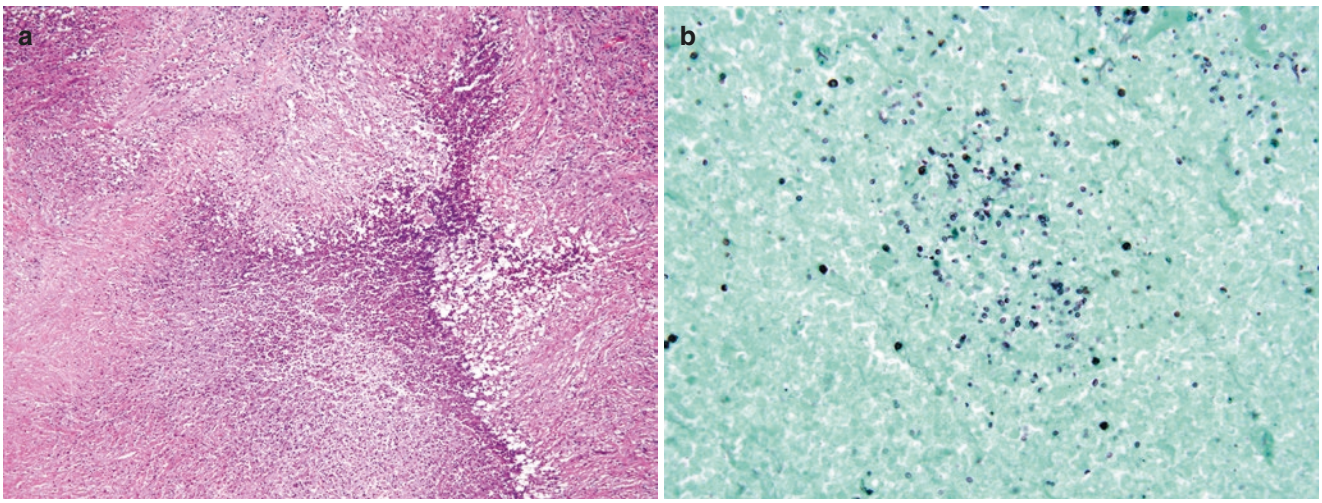

Fig. 4.23 Histoplasmosis. (**a**) The necrotizing granulomatous inflammation in acute histoplasmosis as illustrated in this low-magnification photomicrograph can include irregular (geographic) zones of necrosis with nuclear debris resembling the granulomatous inflammation more typical of granulomatosis with polyangiitis (Wegener's granulomatosis). (**b**) A GMS stain reveals small, frequently teardrop-shaped yeasts of *Histoplasma capsulatum*

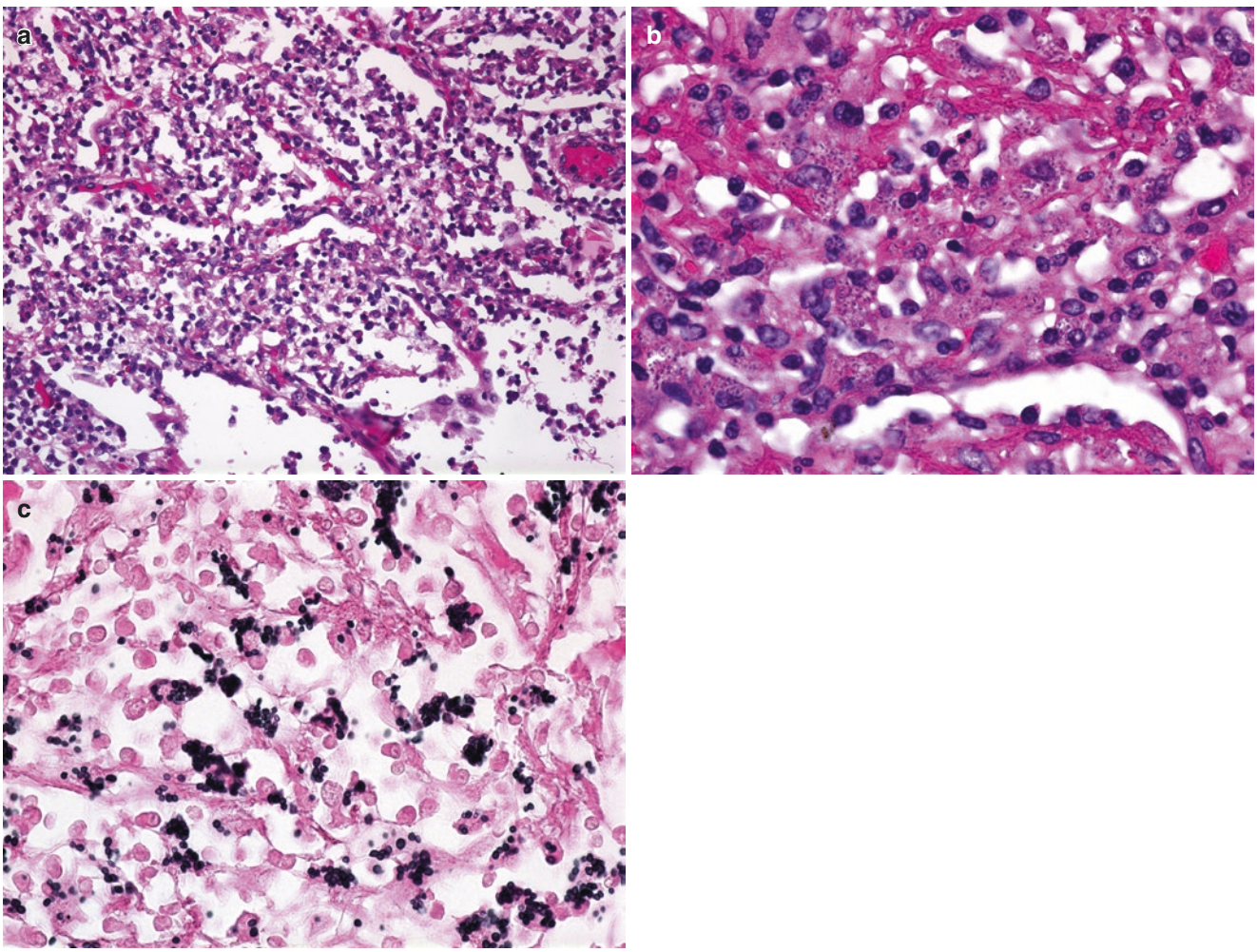

Fig. 4.24 Disseminated histoplasmosis. (**a**) Photomicrograph showing disseminated histoplasmosis characterized by sheets of histiocytes filling air spaces without well-formed granulomas. (**b**) A higher-magnification photomicrograph shows "parasitized" organisms filling the cytoplasm of engorged histiocytes. Yeasts within the cytoplasm of macrophages are visible as dot-like nuclei surrounded by a clear space. This is the only form of histoplasmosis in which you can see the organisms on routinely stained sections. (**c**) High-magnification view of a GMS stain reveals numerous small round and oval-shaped yeasts clustered within the cytoplasm of histiocytes

Blastomycosis

Blastomycosis (Figs. 4.25, 4.26 and 4.27), also termed North American blastomycosis, is caused by *Blastomyces dermatitidis* and is endemic in the south and central United States. Blastomycosis occurs in both immunocompetent and immunocompromised patients. Like other endemic fungal diseases included in this section, blastomycosis has several different clinical phenotypes that extend to involvement of extrapulmonary sites, primarily the skin. Asymptomatic disease is less common compared to histoplasmosis. Yeast forms are morphologically characteristic and are visible on H&E-stained sections.

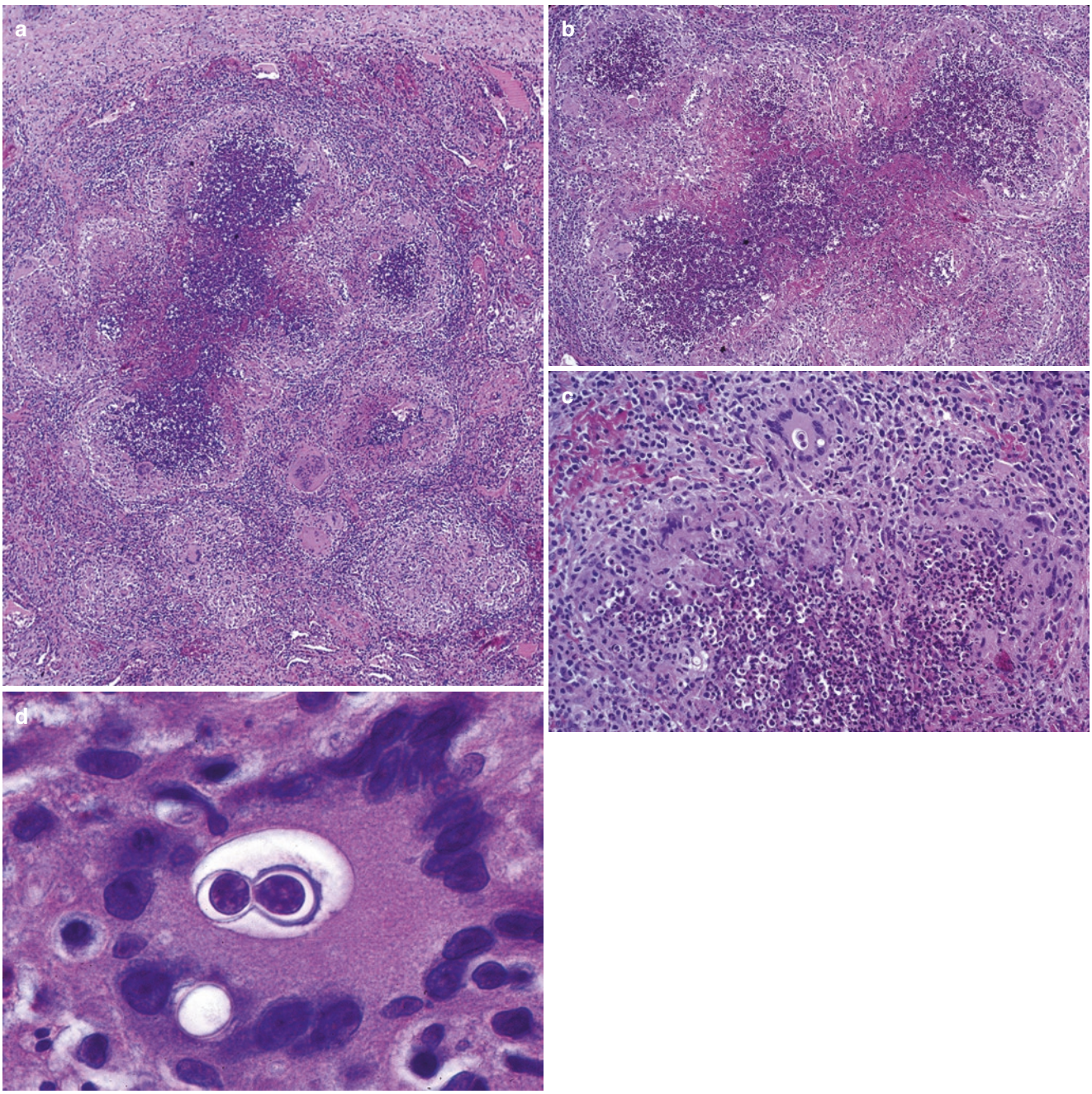

Fig. 4.25 Blastomycosis. (**a**) Low-magnification photomicrograph showing a combination of necrotizing and non-necrotizing granulomatous inflammation in a patient with blastomycosis. (**b**) A higher-magnification view shows suppurative granulomatous inflammation that is characteristic of blastomycosis. The central necrosis shows abundant neutrophils with karyorrhexis surrounded by plump epithelioid histiocytes and giant cells. (**c**) Photomicrograph from the same biopsy showing a budding yeast form in a giant cell in the upper center portion of the image. (**d**) High-magnification view of the same budding yeast showing characteristic doubly refractile wall and central basophilic nucleoplasm. A second organism is present below and to the left in the same giant cell but lacks the central basophilic nucleoplasm

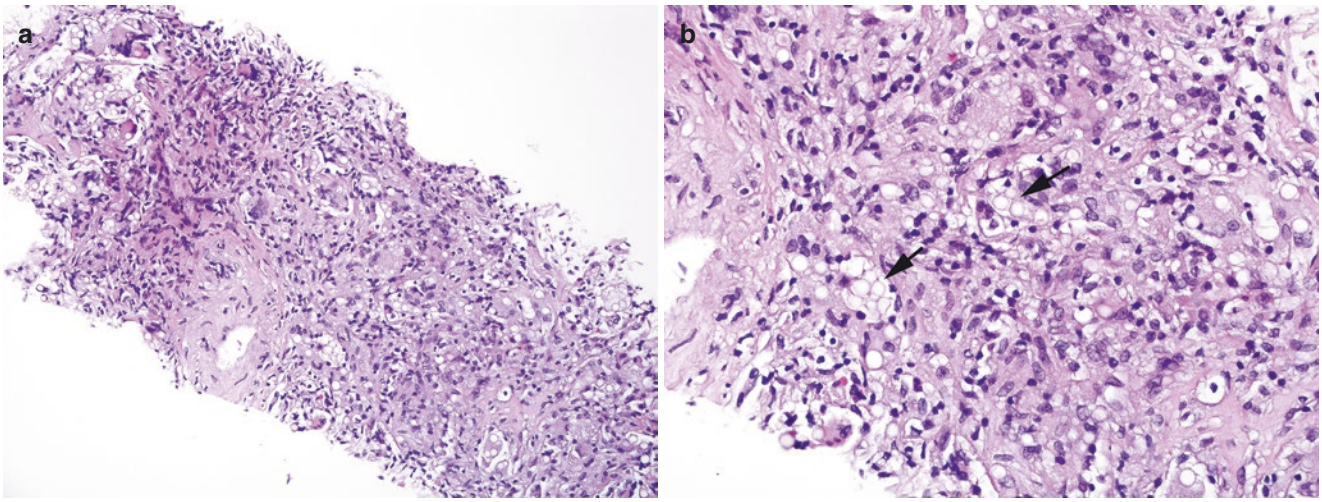

Fig. 4.26 Blastomycosis. (**a**) Low-magnification photomicrograph of a needle biopsy from a solitary lung nodule showing poorly formed non-necrotizing granulomas including multinucleated giant cells. (**b**) High-magnification view showing multiple large, rounded yeasts with thick, refractile cell walls (arrows). Some yeasts show broad-based budding. The organisms are larger than *Cryptococcus neoformans* with which they may be confused and lack the central endospores typical of *Coccidioides immitis*

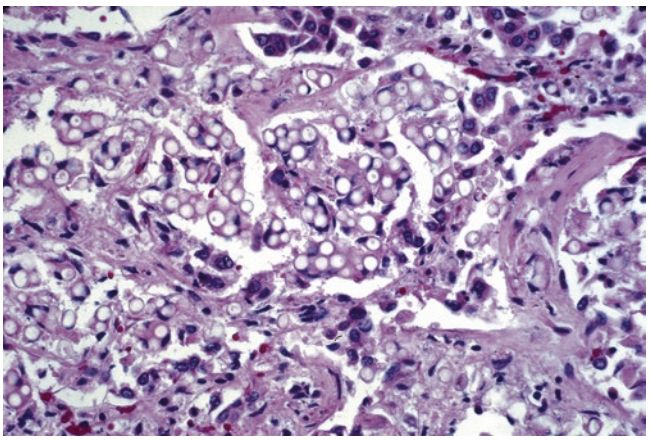

Fig. 4.27 Blastomycosis in the acute respiratory distress syndrome (ARDS). Photomicrograph of autopsy lung showing numerous round yeasts with thick doubly refractile walls typical of *Blastomyces dermatitidis* with diffuse alveolar damage. This is an uncommon manifestation of blastomycosis that occurs most commonly in immunocompromised patients

Cryptococcosis

Cryptococcosis (Figs. 4.28, 4.29, 4.30 and 4.31) may affect immunocompetent hosts, but symptomatic disease occurs more commonly in patients who are immunocompromised or have other underlying comorbidities. *Cryptococcus neoformans* has a worldwide distribution with no geographically defined variation in incidence. Patients with cryptococcal infections may be asymptomatic or may have a range of respiratory syndromes, including a subset with isolated lung nodules and ipsilateral nodal disease mimicking tuberculosis or histoplasmosis. In its classic form, *Cryptococcus neoformans* is distinguished by a mucicarminophilic capsule, but capsule-deficient strains lack this feature.

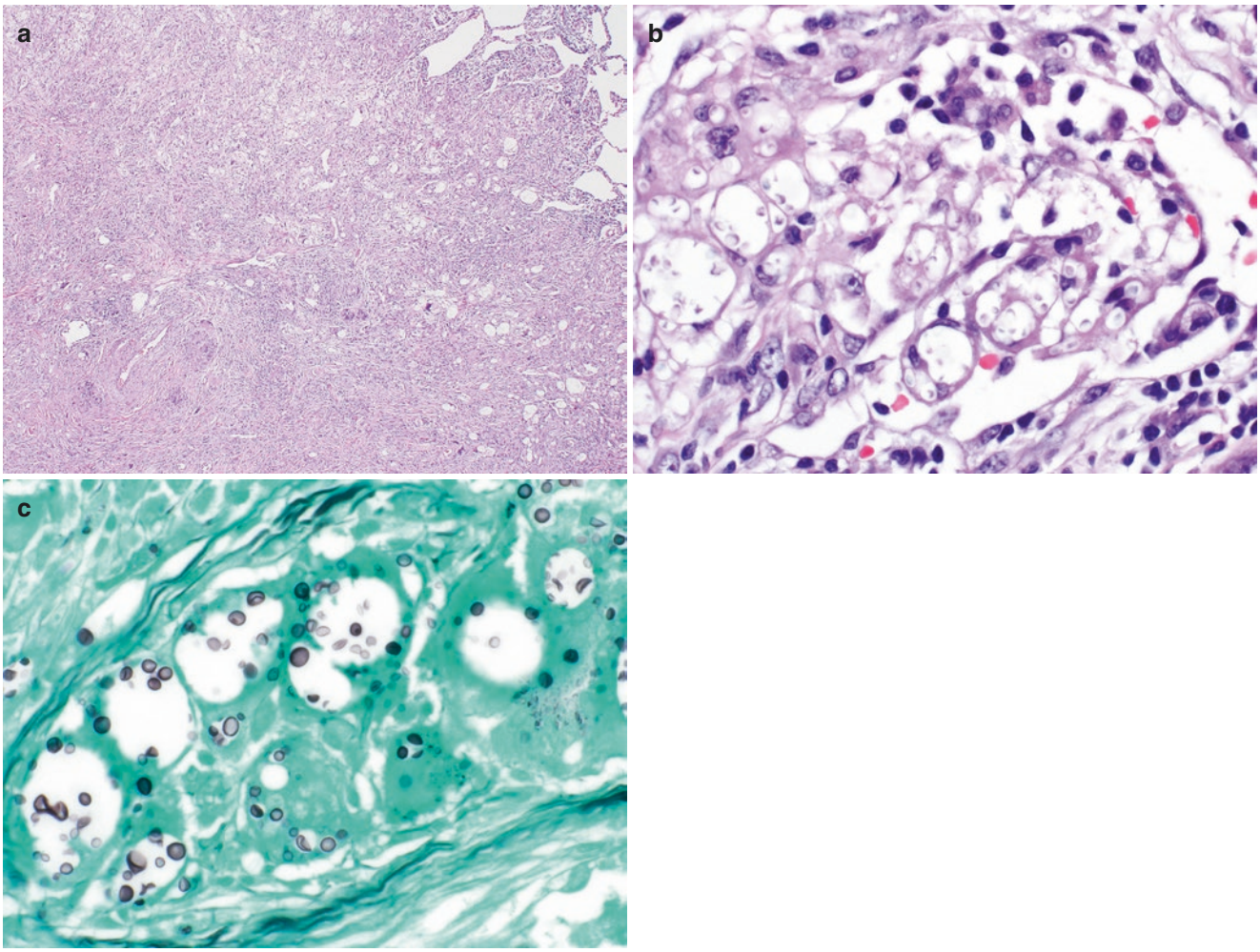

Fig. 4.28 Cryptococcosis. (**a**) Low-magnification photomicrograph showing a nodule in which poorly formed non-necrotizing granulomas comprise loose clusters of multinucleated giant cells with variably conspicuous cytoplasmic vacuoles. (**b**) High-magnification view showing that many of the cytoplasmic vacuoles contain delicate, pale-staining, thin-walled yeast with associated halos representing mucinous capsules. (**c**) High-magnification photomicrograph of GMS stain showing the round and misshapen fractured yeast forms typical of *Cryptococcus neoformans*

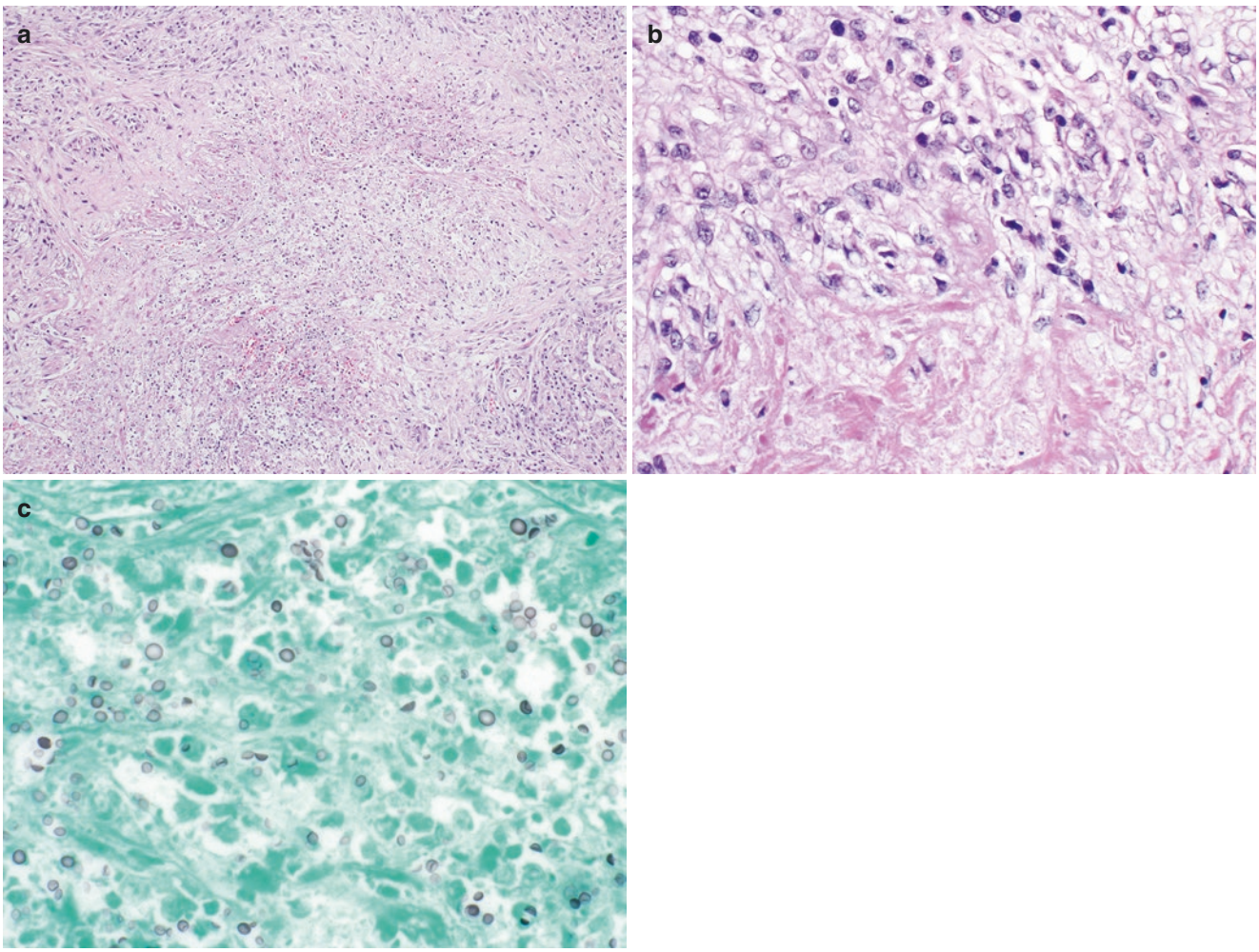

Fig. 4.29 Cryptococcosis. (**a**) Photomicrograph showing necrotizing granuloma that contributed to the same nodule illustrated in Fig. 4.28. This combination of necrotizing granulomas and loose clusters of multinucleated giant cells is a common tissue manifestation of pulmonary cryptococcosis. (**b**) Higher-magnification view showing necrotic center of granuloma at the bottom surrounded by a mixed inflammatory infiltrate of mononuclear cells in which epithelioid histiocytes predominate. (**c**) High-magnification photomicrograph of GMS illustrating yeast typical of *Cryptococcus neoformans* randomly scattered with the necrotic center of the granuloma

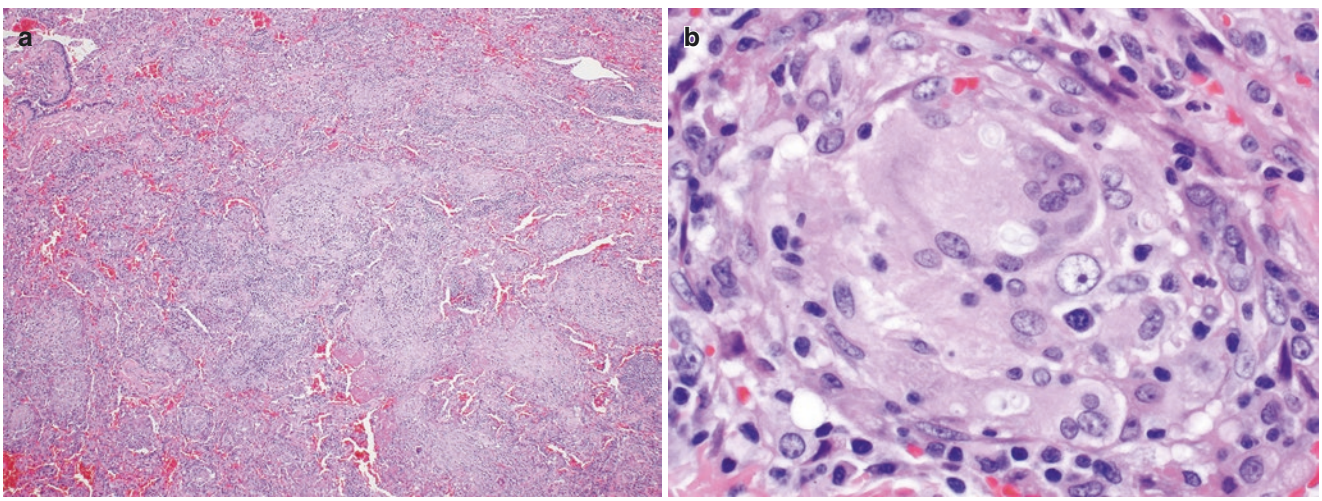

Fig. 4.30 Cryptococcosis. (**a**) Organizing pneumonia is a common manifestation of cryptococcosis, as illustrated in this low-magnification photomicrograph. It is distinguished by associated granulomatous inflammation, including clusters of epithelioid and multinucleated macrophages. (**b**) High-magnification view showing the delicate, pale-staining, thin-walled yeast with associated halos that are the histologic hallmarks of *Cryptococcus neoformans*

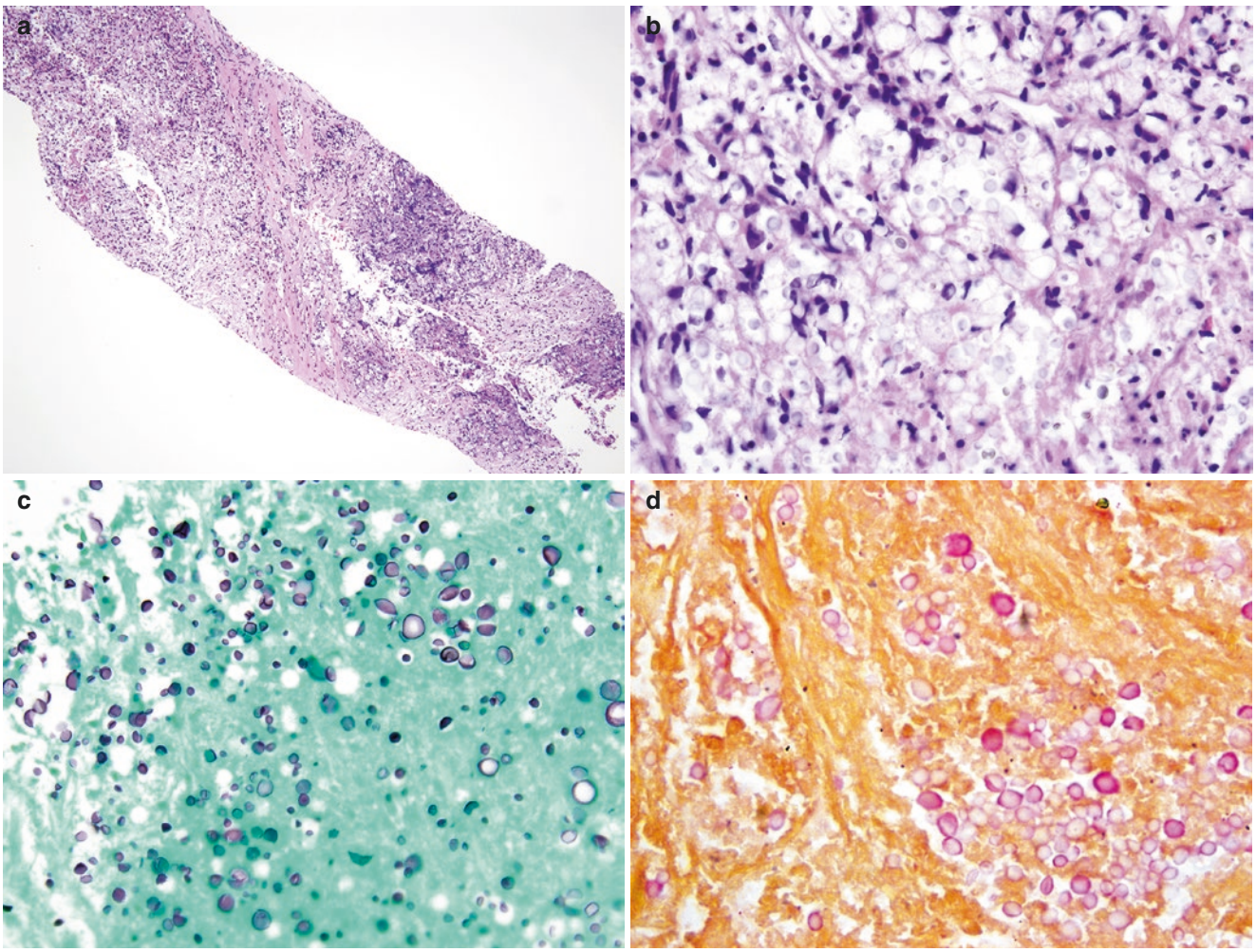

Fig. 4.31 Cryptococcosis. (**a**) Low-magnification photomicrograph of a needle biopsy from a lung nodule in an immunocompromised patient. Areas of pale-colored necrosis and vaguely granulomatous inflammation are seen. (**b**) High-magnification photomicrograph showing the pale-colored necrosis in which there are numerous round yeasts with minimal inflammatory reaction and without well-formed granulomas. The yeasts vary markedly in size and shape and are surrounded by a prominent clear space corresponding to a mucinous capsule. (**c**) High-magnification view of the GMS stain highlights the characteristic features of *Cryptococcus*: variation in size and frequent fragmentation of the yeast. (**d**) High-magnification photomicrograph illustrating the brightly mucicarminophilic capsule seen in most (but not all) strains of *Cryptococcus neoformans*. Capsule-deficient strains may lack this characteristic

Coccidioidomycosis

Coccidioidomycosis (Figs. 4.32, 4.33, 4.34 and 4.35) is endemic in the southwestern United States and is caused by the dimorphic fungi *Coccidioides immitis* and *Coccidioides posadasii*. It causes disease in both immunocompetent and immunocompromised patients and may be biopsied or excised because of its tendency to form a localized lung nodule. The organism divides by a process of endosporulation, a feature helpful in identifying *Coccidioides* in routinely and specially stained sections. The mycelial form is much less commonly found in surgical lung specimens.

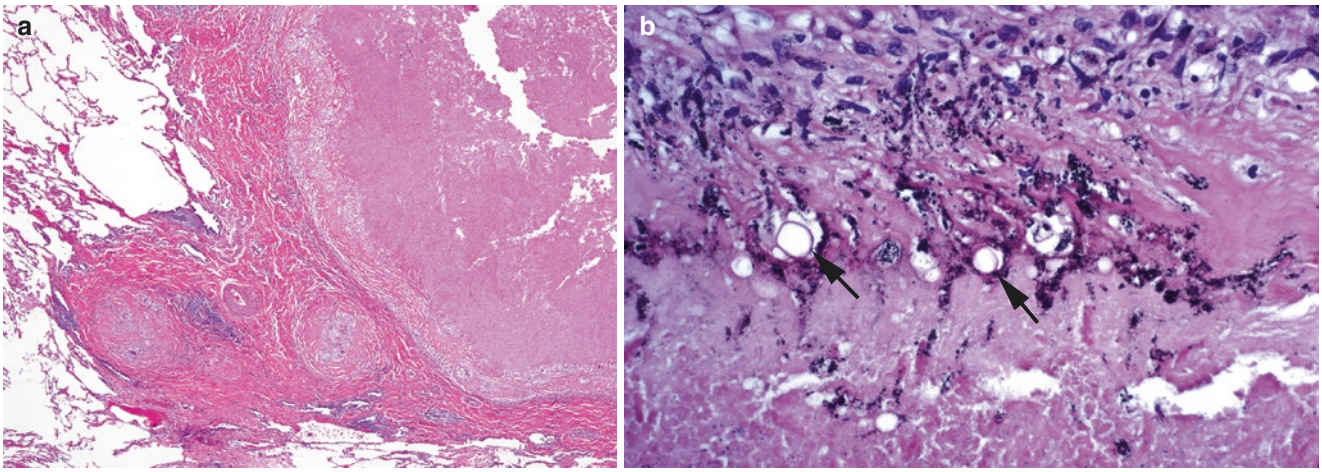

Fig. 4.32 Coccidioidomycosis. (**a**) Necrotizing granulomatous inflammation is the most common finding in *Coccidioides* infections. This low-magnification photomicrograph shows a large area of bland necrosis surrounded by epithelioid histiocytes and giant cells with non-necrotizing granulomas at the periphery. (**b**) High-magnification photomicrograph showing large empty spherules (arrows) with a thick, somewhat refractile wall at the edge of necrosis. Note that the spherules are much larger than adjacent histiocytes

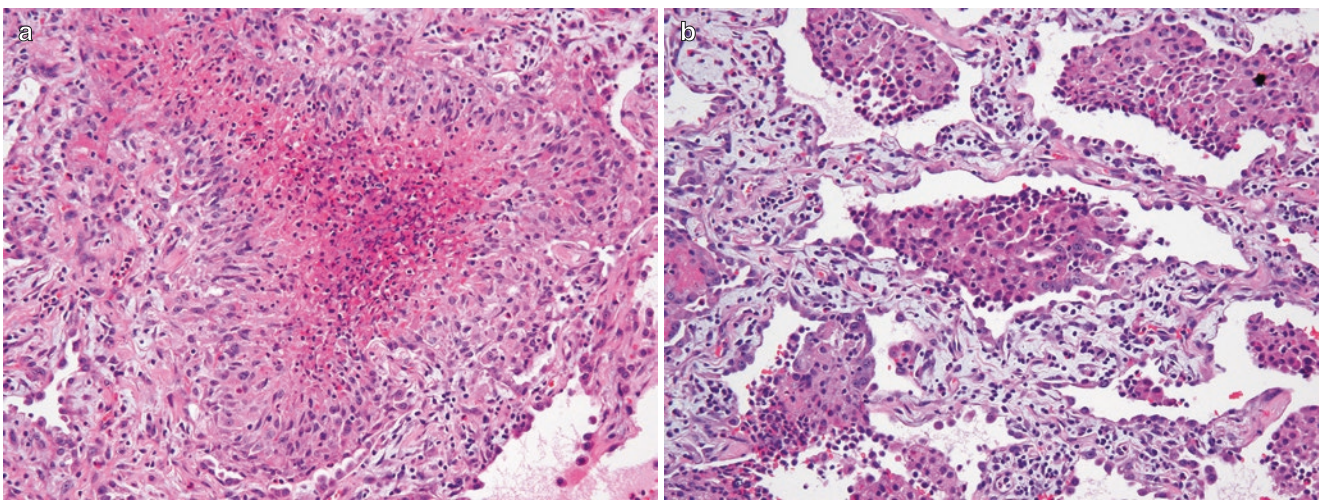

Fig. 4.33 Coccidioidomycosis with eosinophilia. (**a**) Photomicrograph showing necrotizing granuloma with associated eosinophilia in a patient with coccidioidomycosis. Tissue eosinophilia is commonly associated with necrotizing granulomatous inflammation in coccidioidomycosis and may include areas resembling eosinophilic pneumonia, as illustrated in the same biopsy in (**b**)

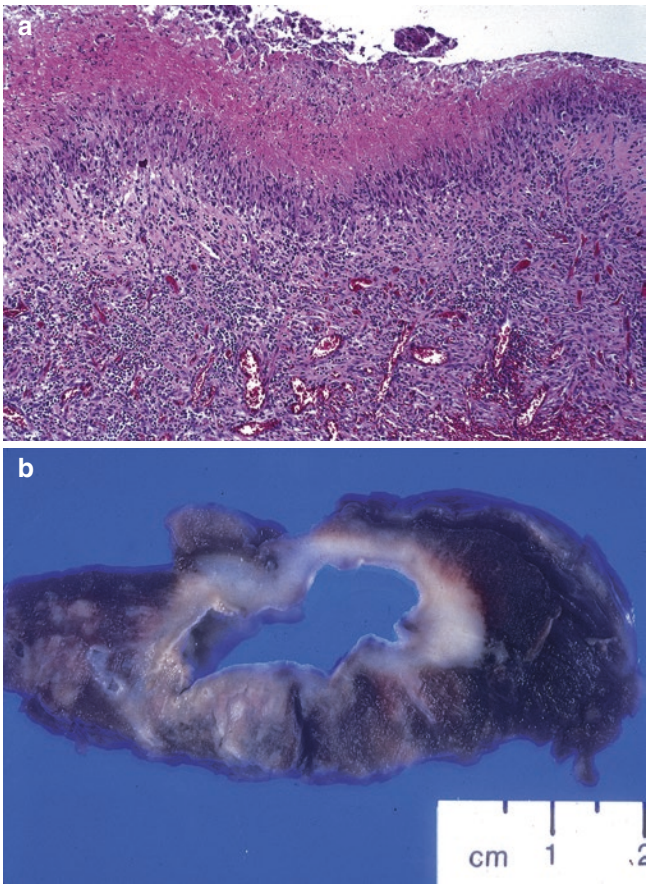

Fig. 4.34 Cavitary coccidioidomycosis. (**a**) This low-magnification photomicrograph illustrates necrotizing granulomatous inflammation with cavitation in a patient with coccidioidomycosis. (**b**) Photograph of surgical specimen corresponding to photomicrograph in **a** showing a cavitary lesion with an irregular rim of firm inflammatory tissue

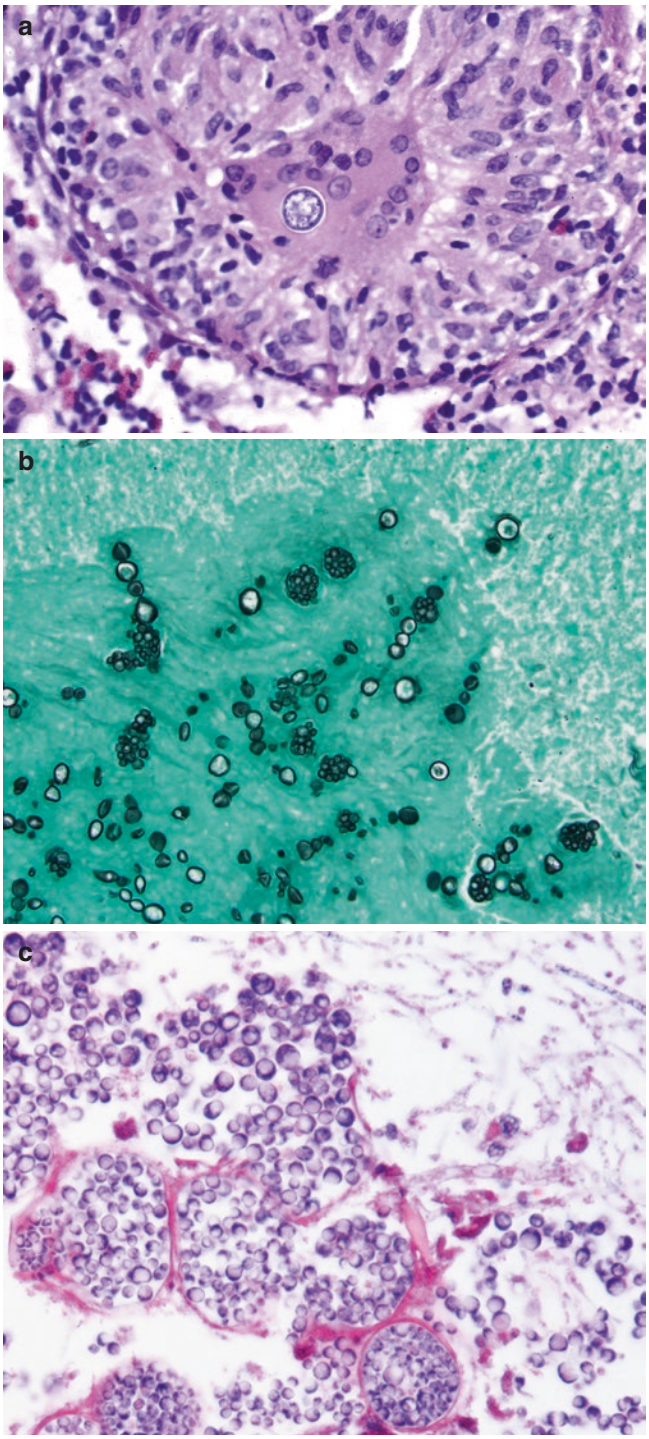

Fig. 4.35 Coccidioidomycosis. (**a**) High-magnification photomicrograph showing a multinucleated giant cell containing a *Coccidioides* spherule with multiple small slightly basophilic endospores. Note the eosinophils in the lower left corner. (**b**) Photomicrograph of a GMS-stained section showing multiple large empty spherules, spherules containing endospores, and free endospores. (**c**) High-magnification photomicrograph of a routinely stained section showing a combination of spherules, endospores, and hyphae (upper right) in a patient with cavitary disease. Hyphae are an uncommon finding in surgical specimens of coccidioidomycosis and represent the mycelial form of the organism

Aspergillus Infections

Aspergillus infections (Figs. 4.36, 4.37, 4.38, 4.39, 4.40 and 4.41) in the lungs can be noninvasive or invasive. The commonly recognized forms include noninvasive mycetoma or *Aspergillus* fungus ball, allergic bronchopulmonary aspergillosis (ABPA), invasive *Aspergillus* pneumonia, and necrotizing tracheobronchitis. Aspergillomas form in immunocompetent patients with underlying cavitary or cystic lung disease. ABPA affects patients with asthma or cystic fibrosis, and invasive forms of the disease occur in immunocompromised patients. Chronic cavitary aspergillosis is a progressive form of disease that has features intermediate between noninvasive and invasive forms of aspergillosis. It is characterized by radiologic progression and tends to occur in patients with underlying comorbidities, particularly chronic lung disease.

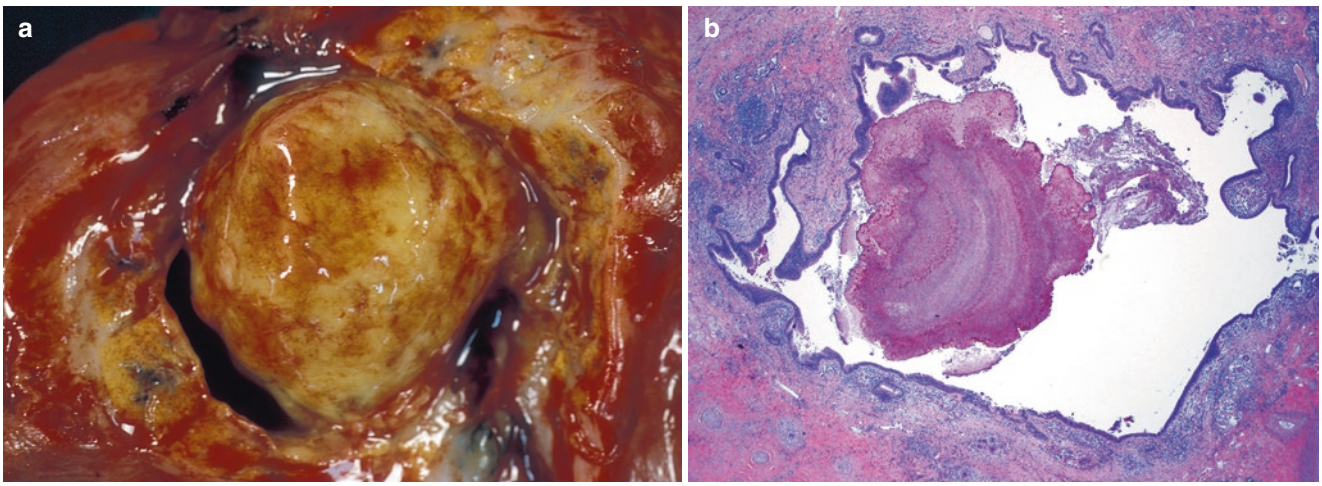

Fig. 4.36 *Aspergillus* mycetoma (aspergilloma). (**a**) Photograph of resected aspergilloma forming a fungus ball within a cavitary space. (**b**) Low-magnification view of fungus ball situated within a dilated airway. Note that there is no tissue response or invasion by the fungus ball

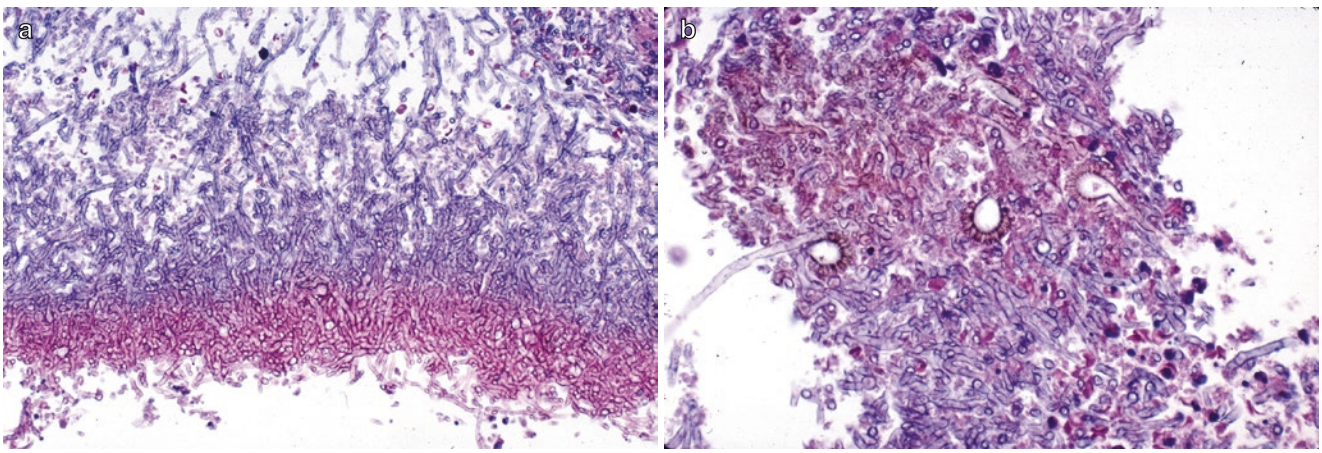

Fig. 4.37 *Aspergillus* hyphae. (**a**) Photomicrograph of routinely stained H&E section showing the organisms comprising an aspergilloma arranged as radially aligned elongated septate hyphae with acute-angle branching. (**b**) High-magnification photomicrograph showing the conidial heads that are occasionally seen and may be helpful in identifying the specific species of *Aspergillus*

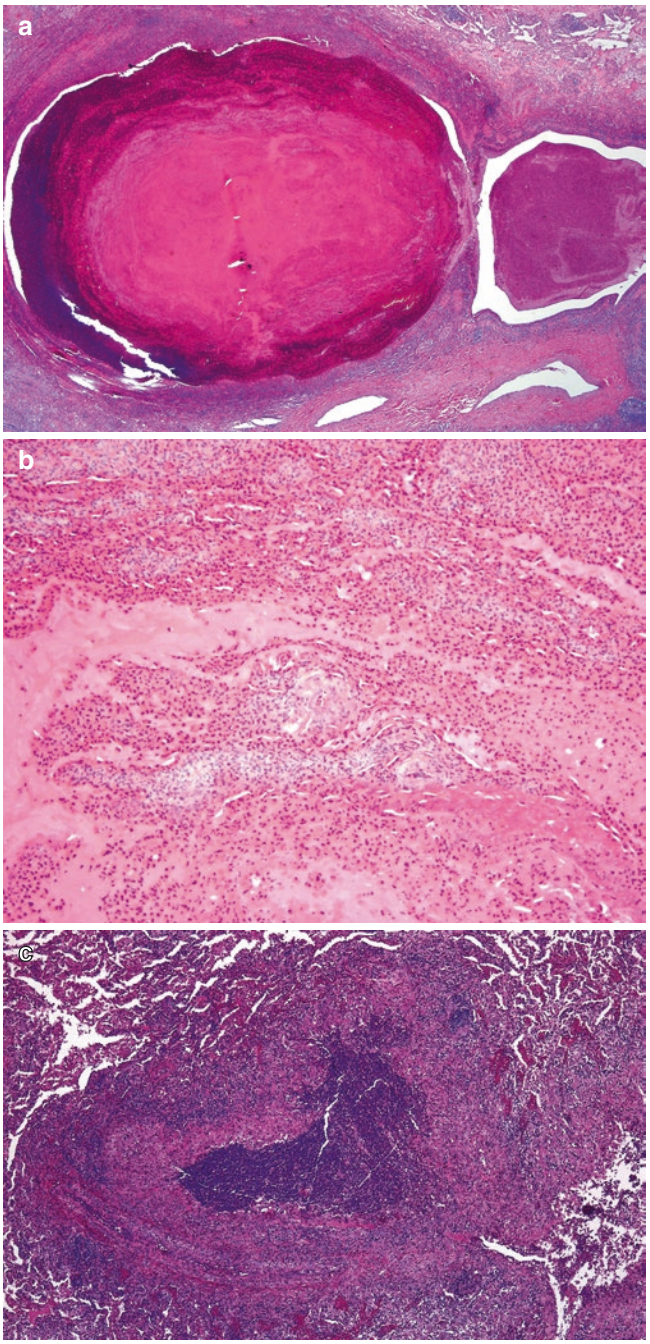

Fig. 4.38 Allergic bronchopulmonary aspergillosis (ABPA). (**a**) Low-magnification photomicrograph showing dilated bronchus filled up with dense mucus plugs demonstrating a layered appearance typical of mucoid impaction of bronchi (MIB) in ABPA. (**b**) High-magnification view showing that the layers of the "allergic mucin" typical of MIB in ABPA constitute a combination of desiccated eosinophils and inspissated mucus in which there are variably conspicuous Charcot-Leyden crystals. (**c**) Low-magnification photomicrograph showing bronchocentric granulomatosis, a finding that in the context of MIB and eosinophilia is characteristic of ABPA. Bronchocentric necrotizing granulomatous inflammation without other features of ABPA occurs in other conditions, including granulomatosis with polyangiitis (Wegener's granulomatosis) and granulomatous infections

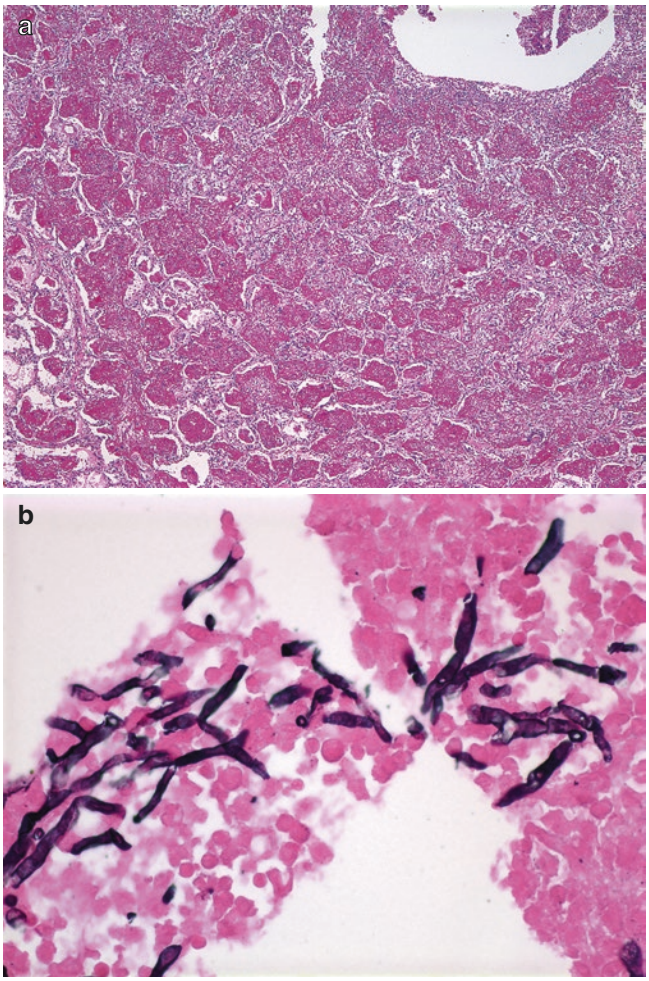

Fig. 4.39 Invasive aspergillosis. (**a**) Low-magnification photomicrograph showing necrotizing pneumonia characteristic of invasive aspergillosis. The air spaces are filled with a fibrinous exudate that includes neutrophils and karyorrhexis. (**b**) High-magnification photomicrograph of GMS-stained section showing fungal hyphae with the necrotizing exudate with branching septate hyphae characteristic of *Aspergillus spp.*

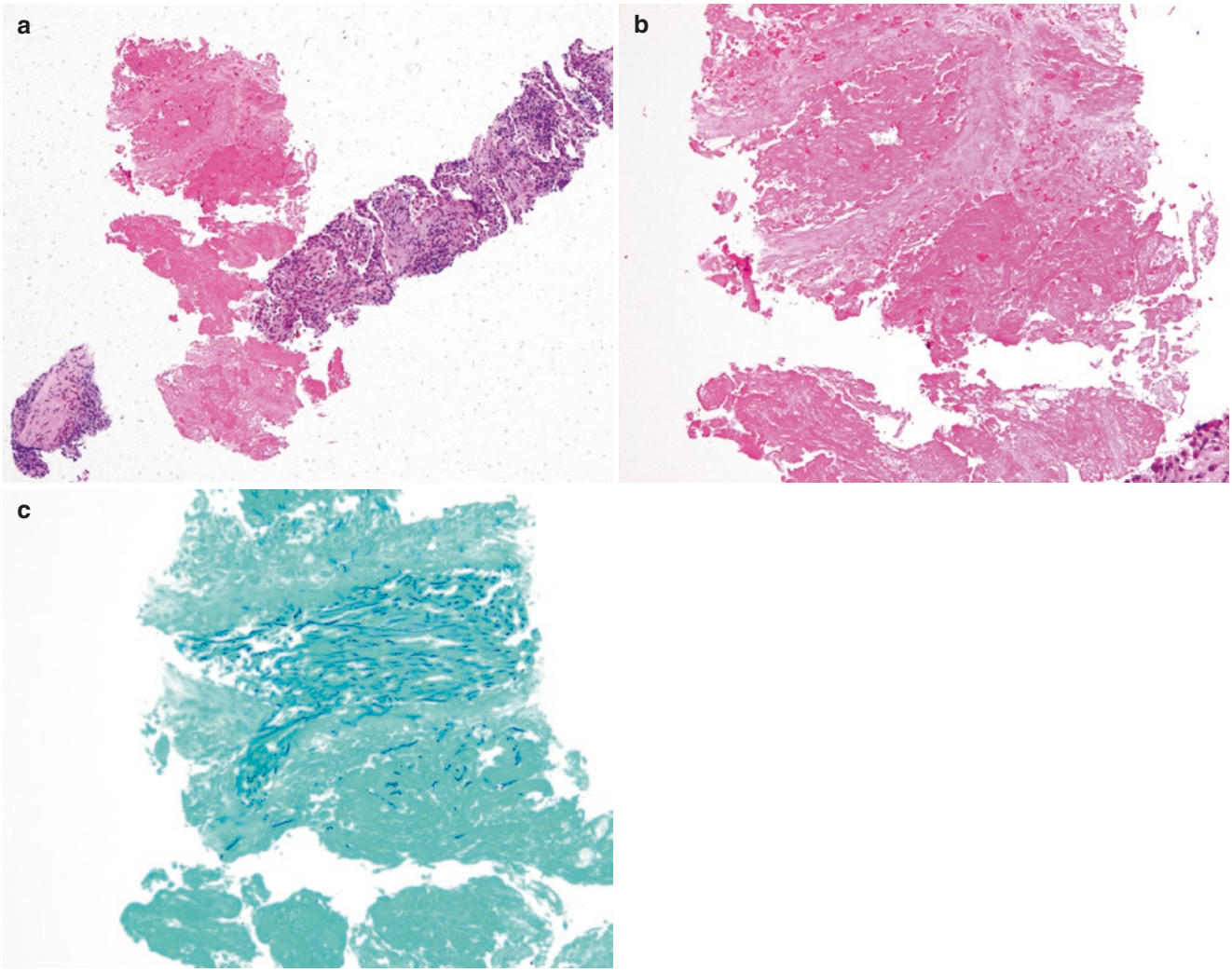

Fig. 4.40 Invasive aspergillosis. (**a**) Low-magnification photomicrograph of a needle biopsy from a lung mass in an immunocompromised patient showing areas of infarction and adjacent organizing pneumonia. (**b**) Higher-magnification view of the infarcted area showing a necrotic blood vessel with questionable fungal hyphae filling up the lumen. (**c**) A GMS stain reveals *Aspergillus* fungal hyphae within the vascular lumen and invading the vascular wall

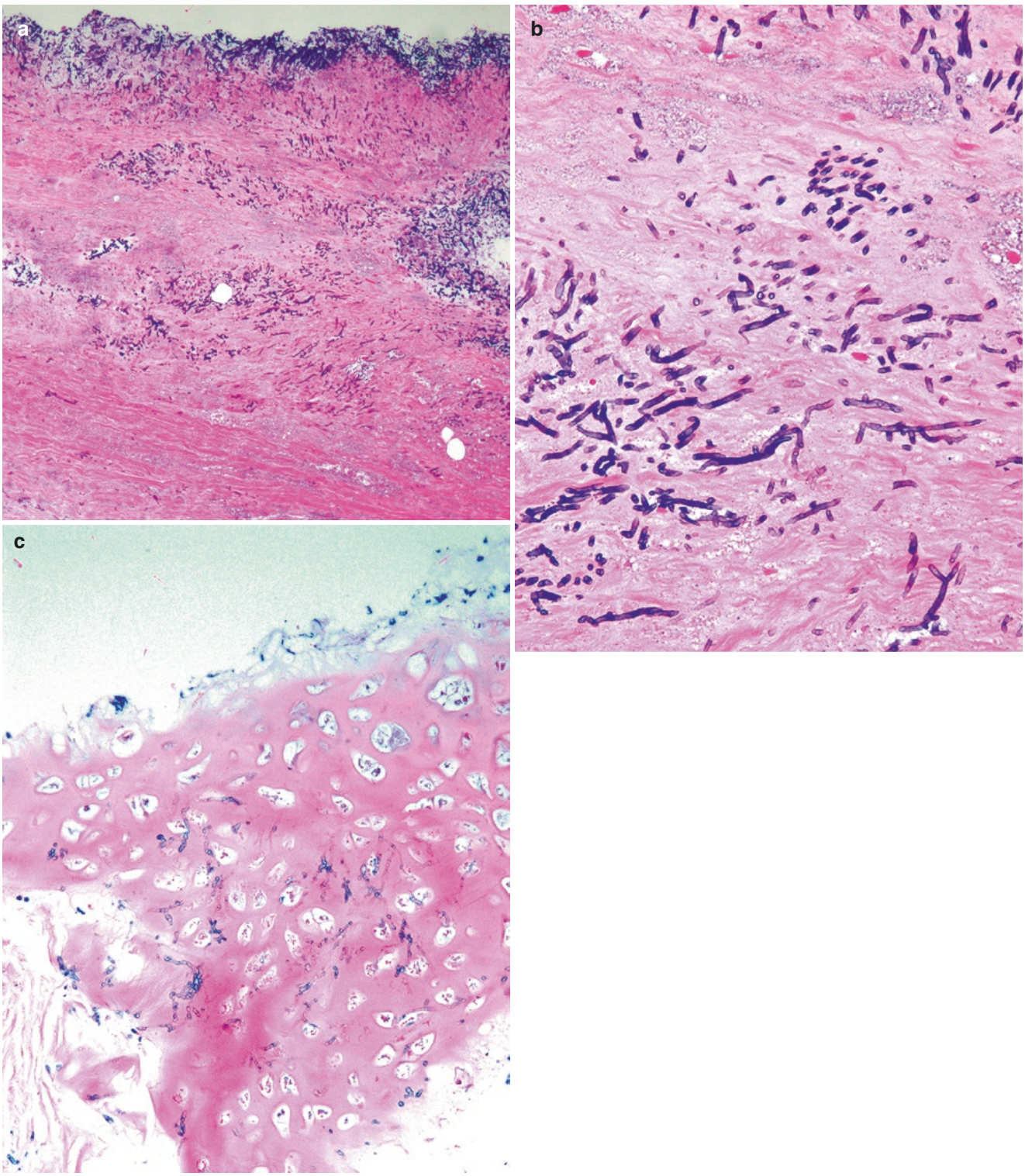

Fig. 4.41 Necrotizing tracheobronchitis as a manifestation of invasive aspergillosis. (**a**) Low-magnification photomicrograph of bronchial wall showing extensive ulceration, necrosis, and invasion by *Aspergillus* fungal hyphae. (**b**) High-magnification photomicrograph of routinely stained section of the bronchial wall showing thin, septate *Aspergillus* hyphae. (**c**) High-magnification view showing extensive invasion of bronchial wall cartilage

Invasive Mucormycosis

Invasive mucormycosis (Figs. 4.42 and 4.43) is caused by a group of fungi referred to as mucormycetes, also referred to as *Mucoromycotina* or *Zygomycota* (zygomycetes). Mucormycosis occurs almost exclusively in immunocompromised patients and frequently involves the lungs. Given the high mortality rate, frozen sections are sometimes requested in order to make a rapid diagnosis and promptly start antifungal therapy.

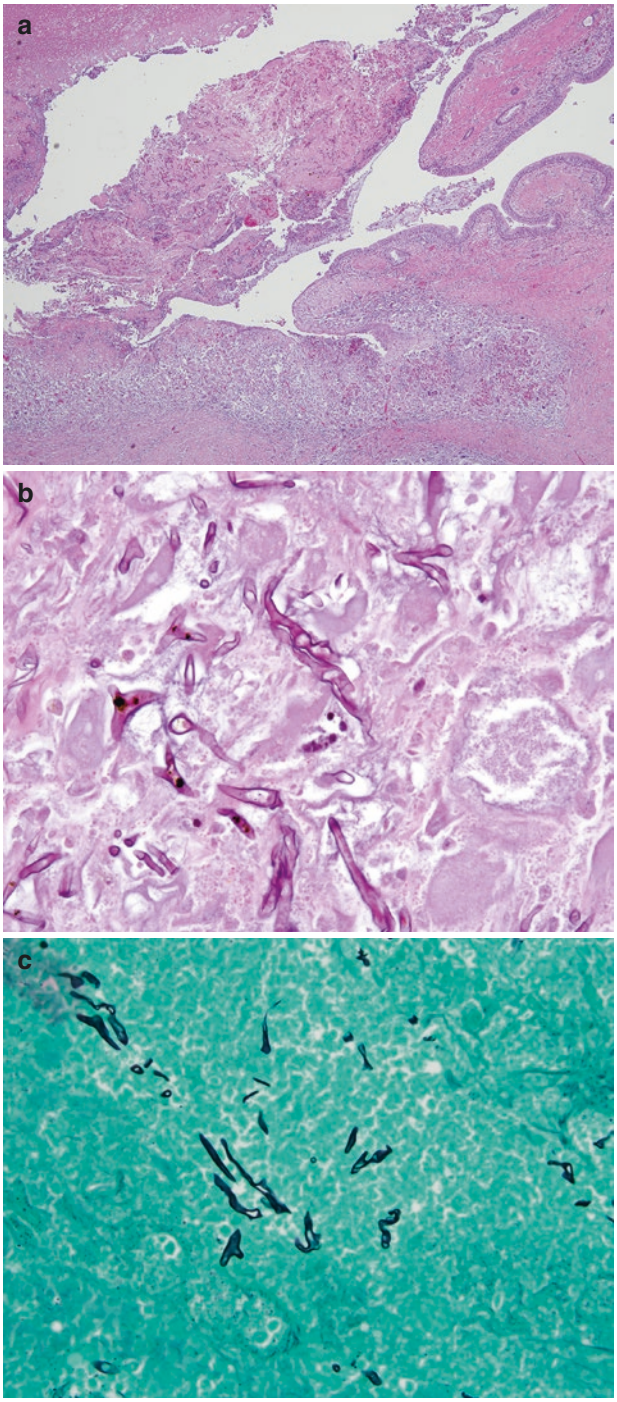

Fig. 4.42 Invasive mucormycosis. (**a**) Low-magnification photomicrograph showing parenchymal necrosis with acute and chronic inflammation, including epithelioid and multinucleated histiocytes resulting in a vaguely granulomatous appearance. Fungal hyphae are present predominantly within the necrotic tissue. (**b**) High-magnification photomicrograph showing the wide, irregular, ribbon-shaped, nonseptate hyphae with 90-degree branching. (**c**) GMS staining showing irregular, ribbon-shaped hyphae with 90-degree branching

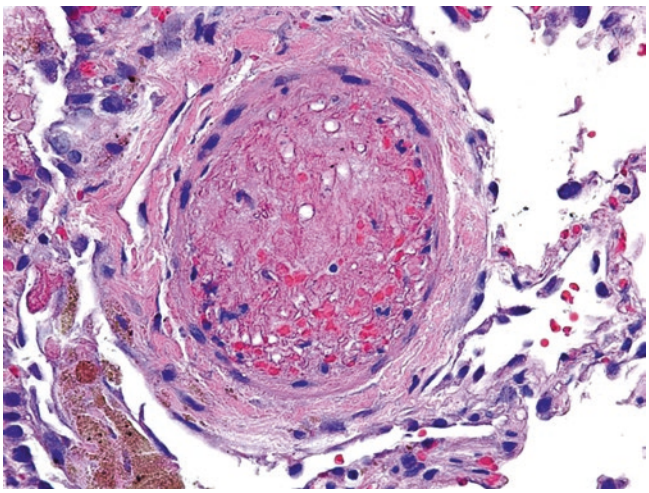

Fig. 4.43 Invasive mucormycosis. High-magnification photomicrograph showing a blood vessel completely occluded by mucor hyphae

Candidiasis

Candidiasis (Figs. 4.44 and 4.45) is rare and occurs primarily in immunocompromised hosts, usually presenting as angioinvasive disease with necrotizing acute bronchopneumonia and abscess formation. Occasionally, candidiasis is more exquisitely localized to blood vessels (intravascular candidiasis). Rarely, the disease is associated with granulomatous inflammation, mainly in patients with underlying chronic granulomatous disease.

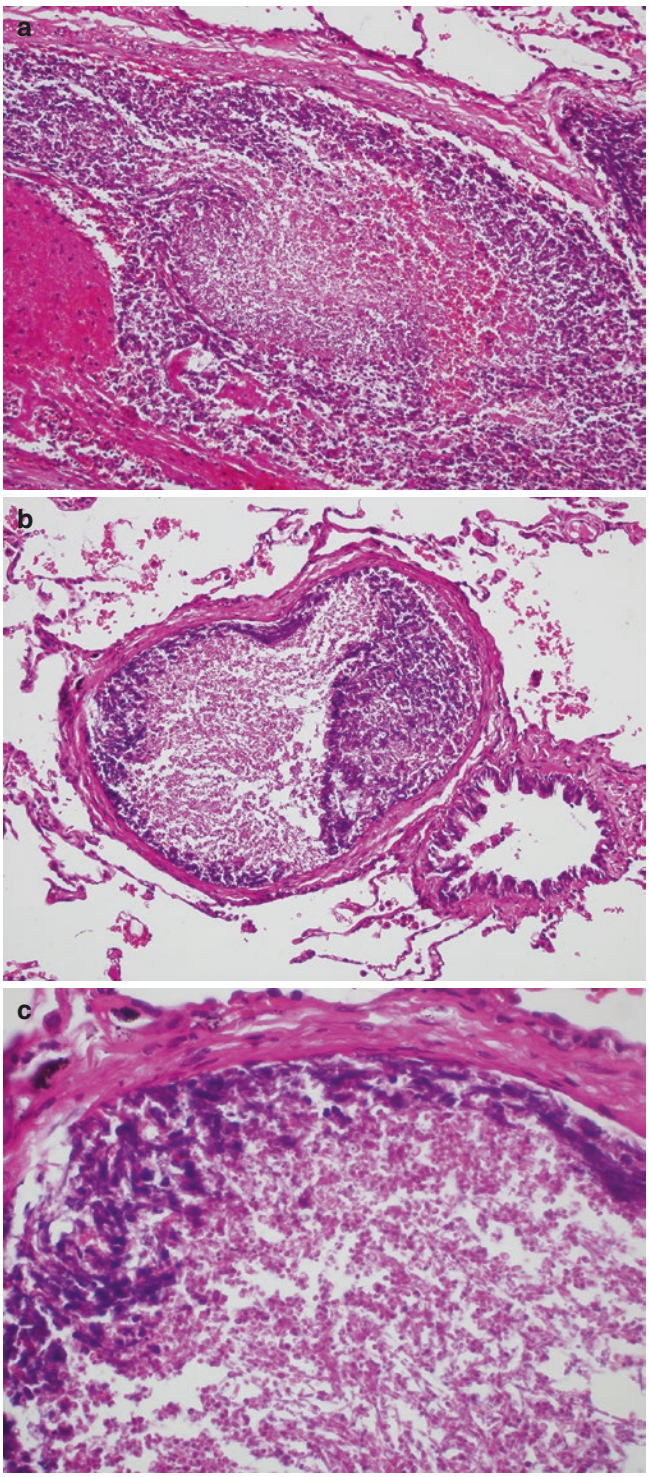

Fig. 4.44 Candidiasis. (**a**) Low-magnification photomicrograph showing blood vessel lumen rimmed by inflammatory cells with a partially necrotic thrombus containing numerous fungal pseudohyphae radially arranged to form a central nidus. (**b**) Low-magnification photomicrograph of a small artery filled with numerous fungal organisms. (**c**) High magnification of the intravascular organisms showing yeasts and pseudohyphae

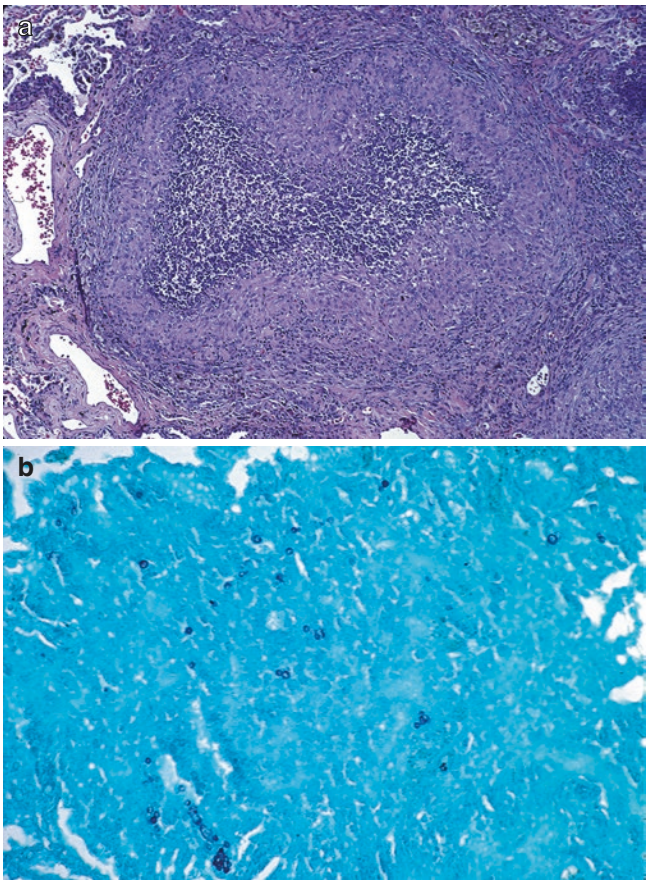

Fig. 4.45 Candidiasis in chronic granulomatous disease. (**a**) Photomicrograph showing suppurative granuloma in a lung biopsy from a patient with chronic granulomatous disease. (**b**) High-magnification photomicrograph of GMS-stained section showing small, narrow-budding yeast in granuloma illustrated above. Cultures grew *Candida spp.*

Pneumocystis Pneumonia

Pneumocystis pneumonia (Figs. 4.46, 4.47, 4.48, 4.49 and 4.50) occurs exclusively in immunocompromised patients. The organism *Pneumocystis jirovecii* was historically considered a protozoon but was reclassified as a fungus on the basis of molecular evidence demonstrating its close relationship to fungi. *Pneumocystis* pneumonia is affiliated with highly variable histologic features and therefore should always be in the differential diagnosis of infections in immunocompromised patients. In its most classic form, the organisms cluster within a fibrinous air-space exudate, producing a characteristic frothy or bubbly appearance on routinely stained sections. Other relatively common variants include granulomatous inflammation and diffuse alveolar damage.

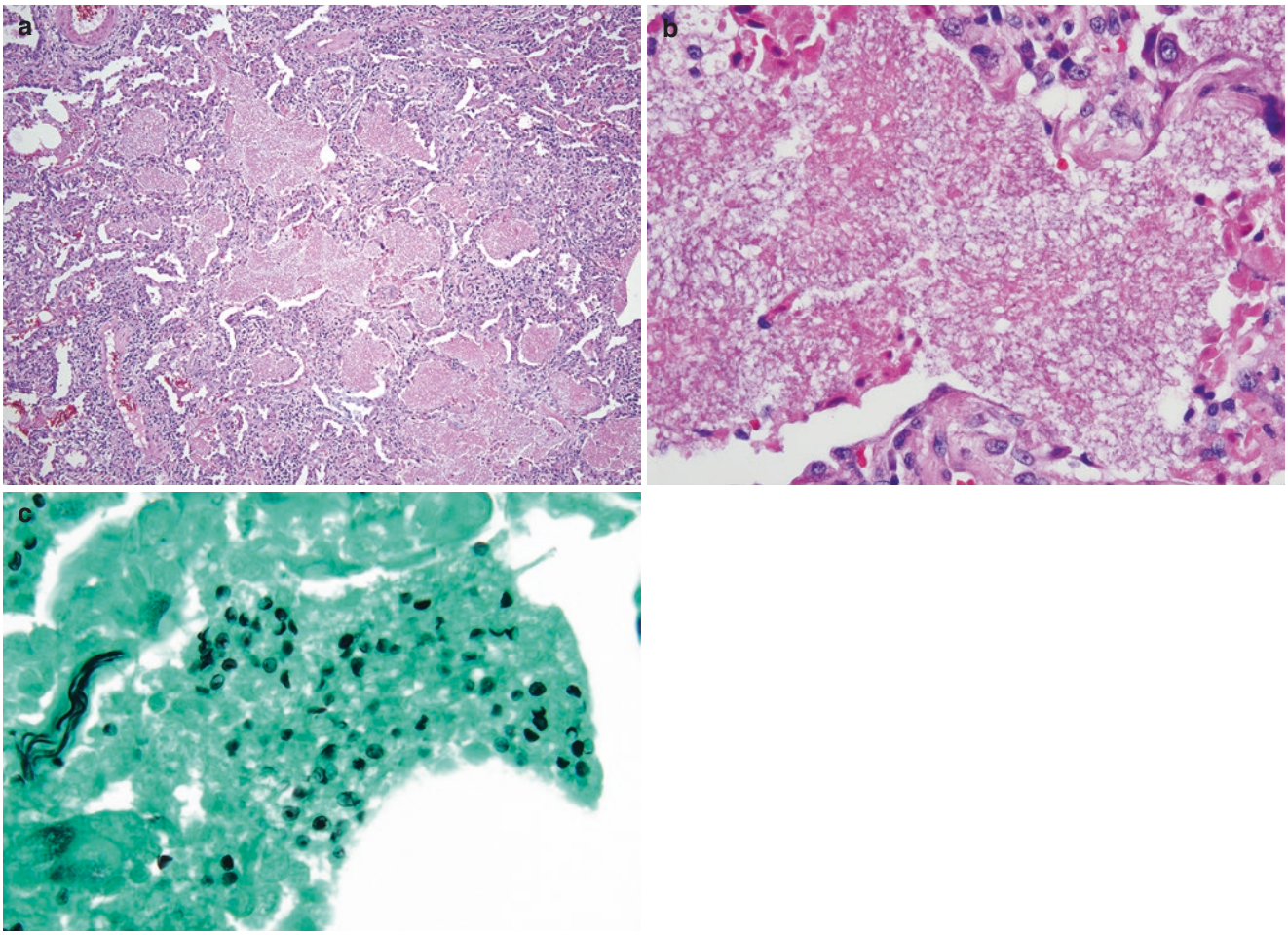

Fig. 4.46 *Pneumocystis* pneumonia. (**a**) Low-magnification photomicrograph of *Pneumocystis* pneumonia showing classic histologic features. The air spaces are filled with frothy eosinophilic exudates. There is nonspecific chronic inflammation within the mildly thickened alveolar septa. (**b**) High-magnification photomicrograph shows the characteristic intra-alveolar frothy exudate. The trophozoites of the organisms, represented by the tiny dot-like structures within the clear space of the frothy materials, are difficult to see on H&E-stained slides but are an important clue to the diagnosis. (**c**) High-magnification view of GMS stain showing numerous round to helmet-shaped cysts within the intra-alveolar frothy exudates. The cysts demonstrate frequent fragmentation and have been described as crushed structures shaped like ping-pong balls. Trophozoites are not visible on GMS-stained slides

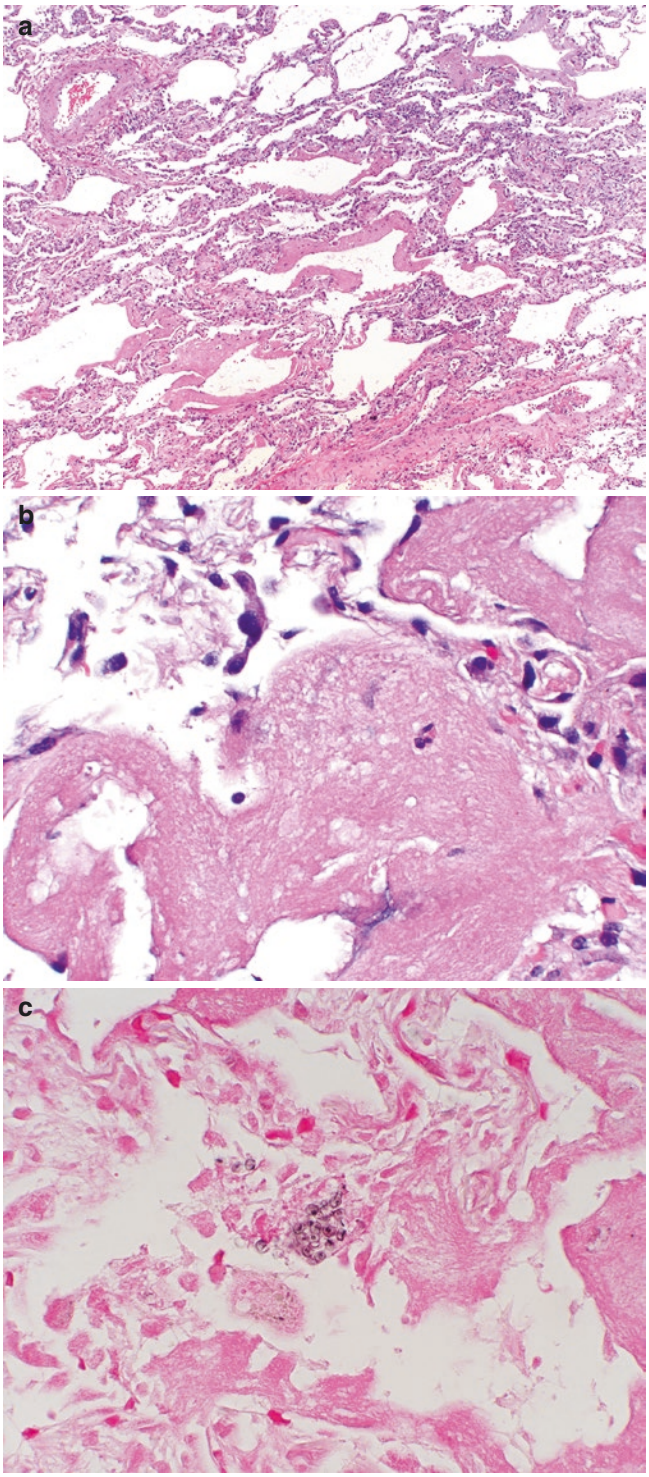

Fig. 4.47 Diffuse alveolar damage is a common manifestation of *Pneumocystis* pneumonia, making a GMS stain mandatory in any immunocompromised patient with this finding. (**a**) Low-magnification photomicrograph of a lung biopsy with *Pneumocystis* pneumonia showing early-stage diffuse alveolar damage with prominent hyaline membranes. (**b**) High-magnification photomicrograph showing the subtle frothy appearance focally present within the lush hyaline membranes. (**c**) High-magnification photomicrograph of GMS-stained section showing organisms typical of *Pneumocystis jirovecii* clustered within the hyaline membranes

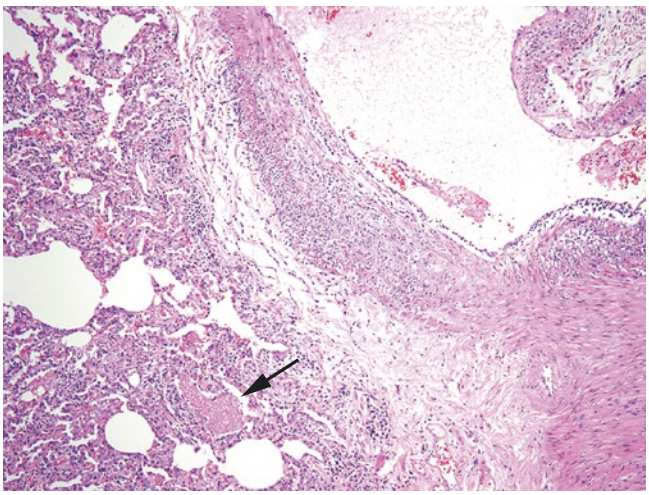

Fig. 4.48 *Pneumocystis* pneumonia. The vasculitis illustrated in this photomicrograph is a rare, atypical finding in *Pneumocystis* pneumonia that may resemble autoimmune or lymphoproliferative diseases. However, the focal presence of the intra-alveolar frothy exudate typical of pneumocystis (arrow) combined with the patient's immunocompromised status are important clues to the diagnosis

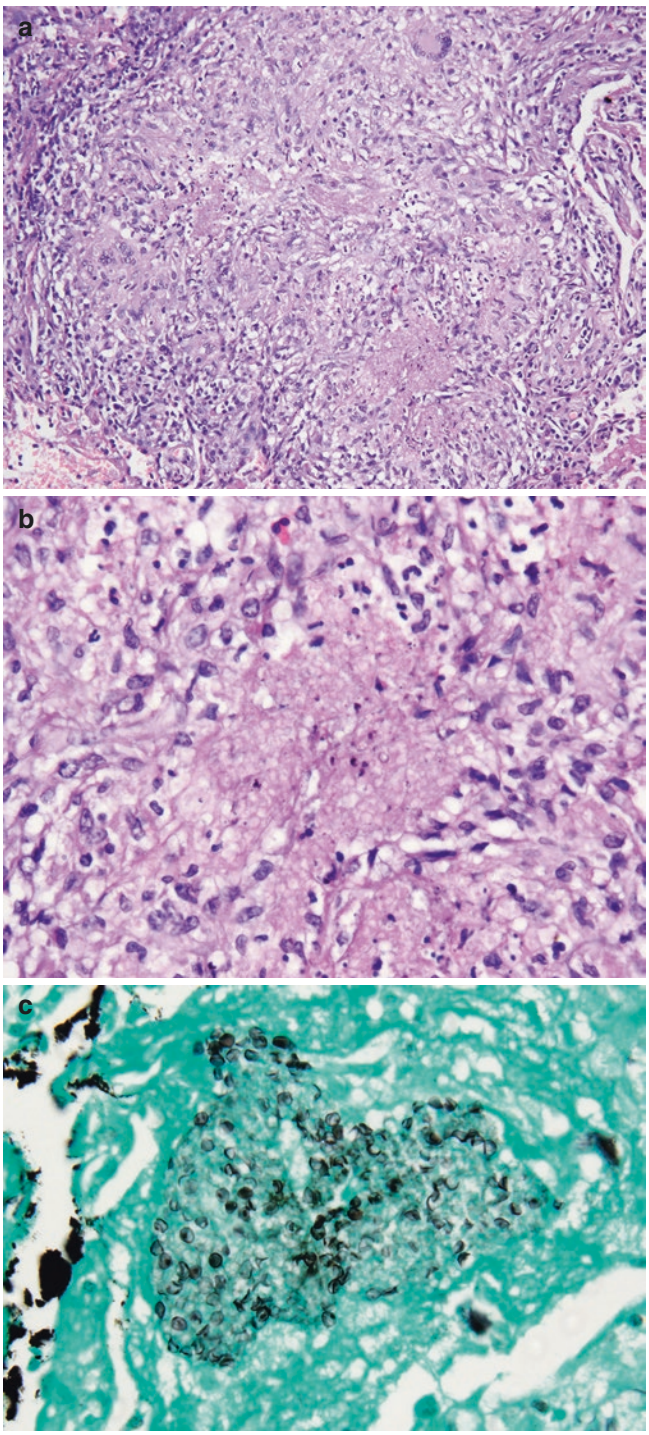

Fig. 4.49 *Pneumocystis* pneumonia. (**a**) Photomicrograph showing granulomatous inflammation in a patient with *Pneumocystis* pneumonia. The poorly formed granulomas are located within the air space. (**b**) Higher-magnification photomicrograph showing the typical frothy exudates that are often only a focal finding when affiliated with granulomatous features. (**c**) High-magnification photomicrograph of GMS-stained section showing numerous round and somewhat fragmented cysts within the central fibrinonecrotic exudates

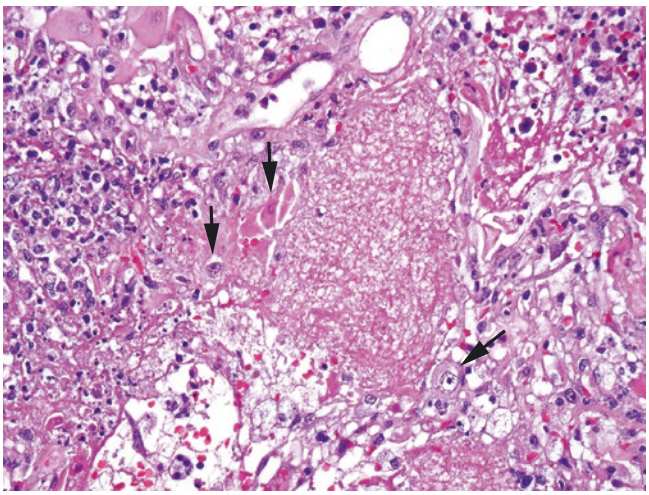

Fig. 4.50 *Pneumocystis* pneumonia with coexisting HSV infection. As illustrated in this high-magnification photomicrograph, more than one organism may be present in a lung biopsy from an immunocompromised patient. This biopsy shows frothy exudates characteristic of *Pneumocystis* pneumonia as well as viral cytopathic changes (arrows) and an associated necrotizing exudate typical of HSV infection

Protozoal and Parasitic Infestations

Protozoal and parasitic infestations (Figs. 4.51, 4.52, 4.53, 4.54, 4.55 and 4.56) in the lungs are rare. Except for dirofilarial nodules, these typically occur in immunocompromised patients.

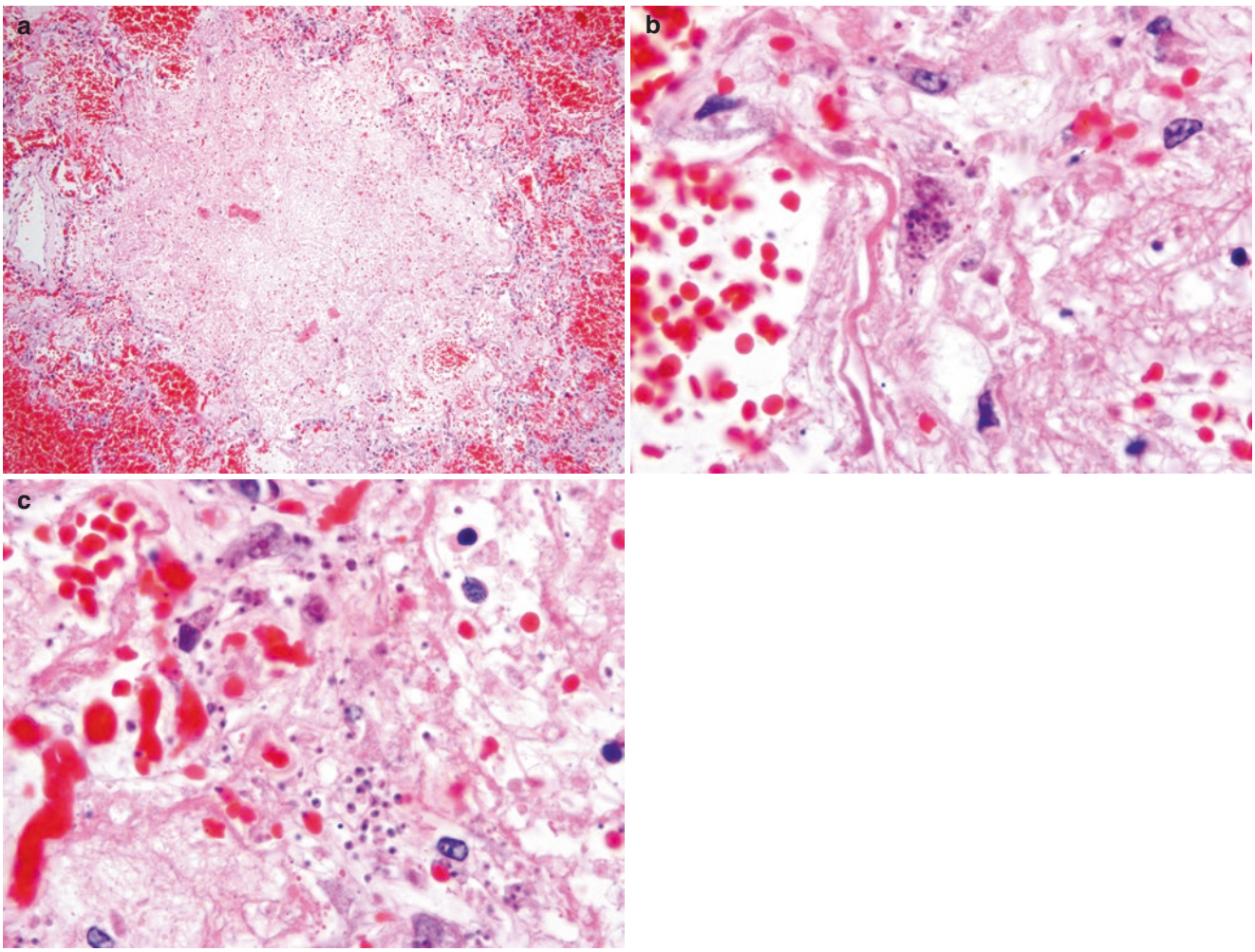

Fig. 4.51 Toxoplasmosis. (**a**) Low-magnification view of a lung biopsy from an immunocompromised patient showing patchy parenchymal necrosis with minimal inflammation. (**b**) High-magnification view at the edge of the necrosis showing an intracellular bradyzoite-containing cyst. (**c**) High-magnification view from elsewhere in the same biopsy showing multiple tachyzoites present within the extracellular exudates

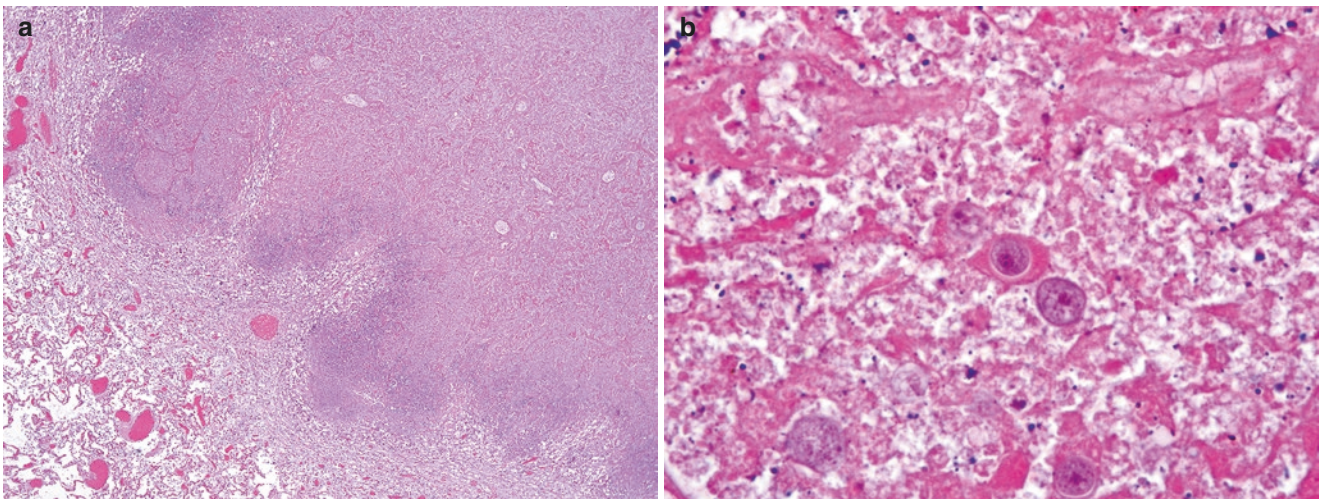

Fig. 4.52 Amoebiasis. (**a**) Low-magnification photomicrograph showing a large, geographic area of necrosis with mild peripheral inflammatory infiltrates. (**b**) High-magnification view at the edge of necrosis showing multiple round to oval trophozoites with a thin cell membrane and single nucleus with prominent nuclear border and central karyosome

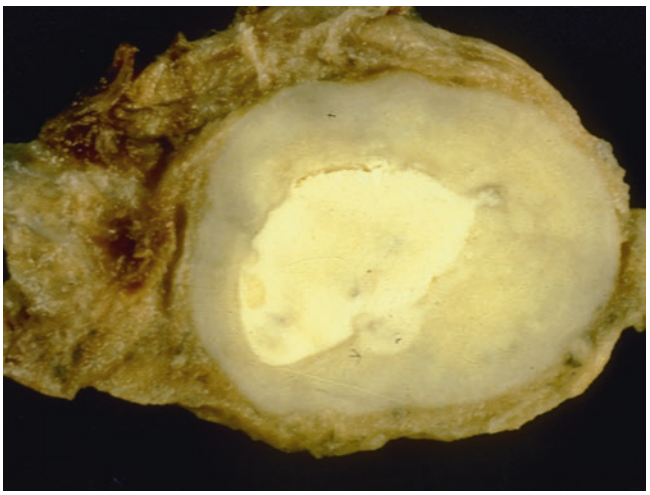

Fig. 4.53 Dirofilarial nodule (dog heartworm disease). Photograph of wedge biopsy from a patient with an asymptomatic solitary nodule showing a solitary well-demarcated centrally necrotic nodule mimicking an infectious granuloma

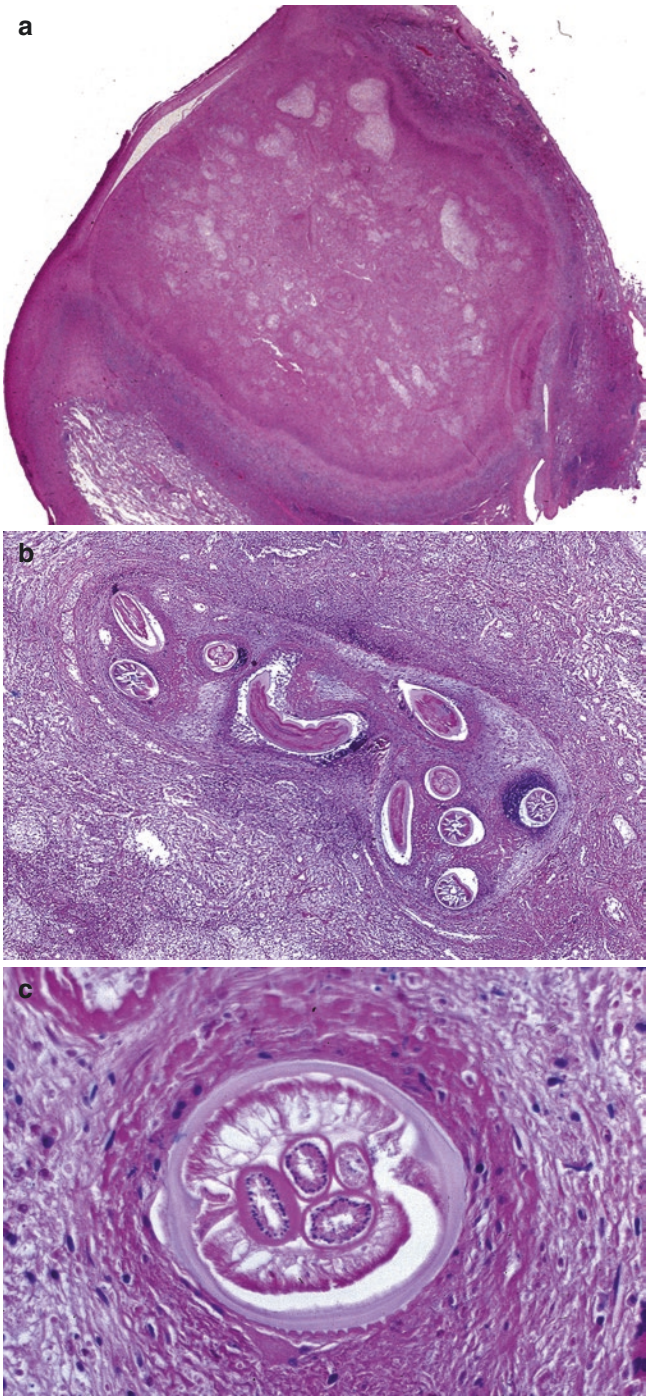

Fig. 4.54 Dirofilarial nodule. (**a**) Low-magnification photomicrograph showing well-circumscribed infarct-like necrosis surrounded by fibrosis and a chronic inflammatory infiltrate rich in eosinophils without well-developed granulomatous features. (**b**) Higher-magnification photomicrograph showing a thrombosed blood vessel containing multiple cross sections of dirofilarial organisms. (**c**) High-magnification view of the organism cut in cross section showing the thick cuticle surrounding complex internal structures

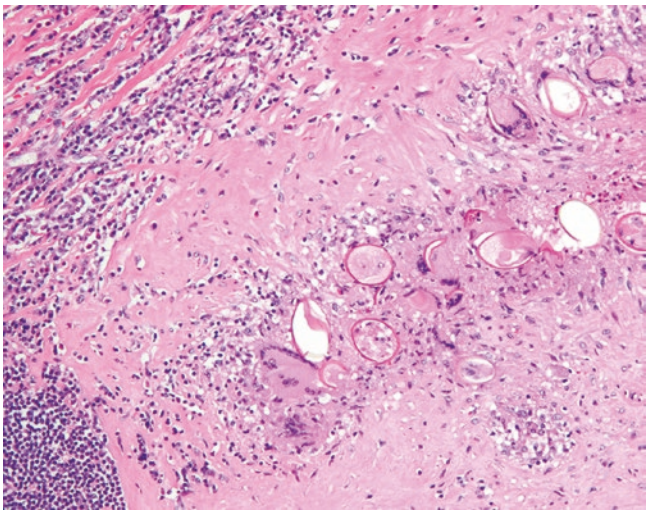

Fig. 4.55 Paragonimiasis (lung fluke). High-magnification view of the wall of a cystic lung lesion showing several oval-shaped eggs with a refractile wall. There are associated fibrosis, chronic inflammation with eosinophils, and multinucleated foreign body giant cells

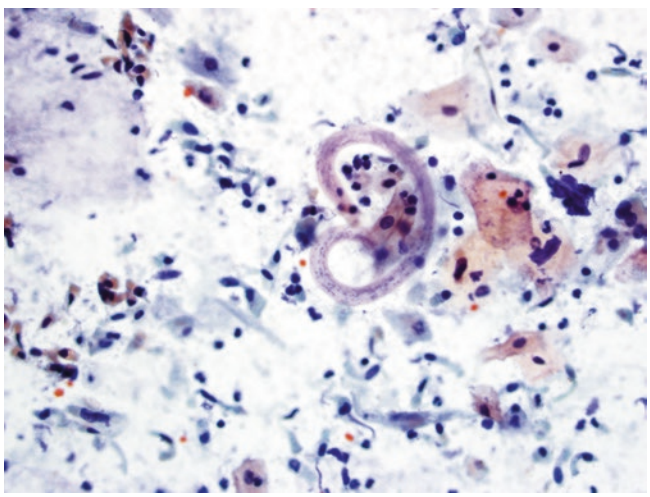

Fig. 4.56 Strongyloidiasis. Papanicolaou stain of bronchoalveolar lavage fluid showing a curved larva of *Strongyloides stercoralis* in a background of mixed inflammation

Suggested Reading

El-Zammar OA, Katzenstein AL. Pathological diagnosis of granulomatous lung disease: a review. Histopathology. 2007;50:289–310.

Gill JR, Sheng ZM, Ely SF, Guinee DG, Beasley MB, Suh J, et al. Pulmonary pathologic findings of fatal 2009 pandemic influenza A/H1N1 viral infections. Arch Pathol Lab Med. 2010;134:235–43.

Hartel PH, Shilo K, Klassen-Fischer M, Neafie RC, Ozbudak IH, Galvin JR, et al. Granulomatous reaction to *Pneumocystis jirovecii*: clinicopathologic review of 20 cases. Am J Surg Pathol. 2010;34:730–4.

Katzenstein A. Unusual pneumonias and granulomatous infections. In: Katzenstein and Askin's surgical pathology of non-neoplastic lung disease. 4th ed. Philadelphia: Elsevier; 2006. p. 261–350.

Kwon KY, Colby TV. *Rhodococcus equi* pneumonia and pulmonary malakoplakia in acquired immunodeficiency syndrome. Pathologic features. Arch Pathol Lab Med. 1994;118:744–8.

Oddo D, Gonzalez S. Actinomycosis and nocardiosis. A morphologic study of 17 cases. Pathol Res Pract. 1986;181:320–6.

Sangoi AR, Rogers WM, Longacre TA, Montoya JG, Baron EJ, Banaei N. Challenges and pitfalls of morphologic identification of fungal infections in histologic and cytologic specimens: a ten-year retrospective review at a single institution. Am J Clin Pathol. 2009;131:364–75.

Travis WD, Pittaluga S, Lipschik GY, Ognibene FP, Suffredini AF, Masur H, et al. Atypical pathologic manifestations of *Pneumocystis carinii* pneumonia in the acquired immune deficiency syndrome. Review of 123 lung biopsies from 76 patients with emphasis on cysts, vascular invasion, vasculitis, and granulomas. Am J Surg Pathol. 1990;14:615–25.

Winn WC Jr, Myerowitz RL. The pathology of the legionella pneumonias. A review of 74 cases and the literature. Hum Pathol. 1981;12:401–22.